DEGREE PROJECT IN MATERIALS DESIGN AND ENGINEERING, SECOND CYCLE, 30 CREDITS

STOCKHOLM, SWEDEN 2020

Experimental study of the temperature profile in an iron ore pellet during reduction using hydrogen gas

JULIA BRÄNNBERG FOGELSTRÖM

KTH ROYAL INSTITUTE OF TECHNOLOGY
SCHOOL OF INDUSTRIAL ENGINEERING AND MANAGEMENT

ABSTRACT

We are facing an important challenge, to reduce the greenhouse gas emissions to make sure that we limit global warming to 2 °C, preferably 1.5 °C. Drastic changes and developing new methods may be our only chance to keep global warming under 1.5 °C. The steel production in Sweden today accounts for 10% of the CO_2 emission. The joint venture HYBRIT (Hydrogen Breakthrough Ironmaking Technology), between SSAB, LKAB and Vattenfall, aims to reduce the CO_2 emission by developing a method that reduces iron ore pellets with hydrogen gas, leaving only water as off-gas.

From simple thermodynamic calculations, it is evident that the reduction of iron ore using hydrogen gas is an endothermic reaction, requiring heat. Based on the calculated energy requirement, the temperature at the center of the pellet should not be the same as the temperature at the surface of the pellet but instead, decrease as the reduction reaction takes place. This report presents the temperature profile at the surface and in the center of a hematite pellet during hydrogen reduction at temperatures of 600 °C, 700 °C, 800 °C and 900 °C. Ideally, the results can be implemented in a model to better simulate the reduction reaction taking place inside a hematite pellet. The experiment consists of three sub-experiments, the first measures the temperature profile of the unreduced iron ore pellet in an argon gas atmosphere, secondly, the temperature profile and mass loss are measured during reduction, lastly, the temperature profile is measured for the reduced pellet in a hydrogen atmosphere. The mass loss measured during hydrogen reduction is used to calculate the degree of reduction.

The results show that the reaction rate increases with increasing temperature and concentration of H_2. Additionally, a higher reduction temperature gives the largest temperature decrease inside the pellet during reduction. At 900 °C, the temperature decrease is equal to 39 °C and at 600 °C, it is equal to 3 °C. The results prove that after a certain initial stage, gas diffusion and heat conduction through the product layers play important roles in controlling the reaction rate. There is even a period where a plateau of the reduction is observed, the reaction is mostly controlled by heat transfer.

SAMMANFATTNING

Idag står vi inför en viktig utmaning, att minska utsläppen av växthusgaser och se till så att vi inte överskrider 2 °C uppvärmning, helst inte 1.5 °C. För att klara detta krävs drastiska förändringar och utvecklingar av nya metoder kan vara vår enda chans att uppnå 1.5-gradersmålet. Ståltillverkningen i Sverige idag står för 10% av CO_2 utsläppen och för att bidra till att minska utsläppen av CO_2 har företaget HYBRIT, vilket står för Hydrogen Brakethrough Ironmaking Technology, skapats. HYBRIT är en joint venture mellan SSAB, LKAB och Vattenfall som tillsammans vill skapa stål på ett mer miljövänligt sätt. Processen går ut på att reducera järnmalmspellets med hjälp av vätgas för att producera järnsvamp och ge ifrån sig vatten som avgas.

Från enkla termodynamiska beräkningar är det lätt att inse att reduktionen med hjälp av vätgas är en endoterm process, som kräver energi. Det är genom denna kunskap som en kan föreställa sig att reduktionen av järnmalmspellets med hjälp av vätgas kommer bidra till en temperaturminskning. I denna rapport har temperaturprofilen inne i och på ytan av en hematitpellet mätts under tiden som den blivit reducerad med vätgas. Idealt kan resultaten implementeras i en modell för att bättre simulera reduktionsreaktionen som äger rum i en hematitpellets. Fyra olika reduktionstemperaturer har undersökts: 600 °C, 700 °C, 800 °C och 900 °C. Experimenten består av tre del-experiment, först mäts temperaturprofilen av den oreducerad hematitpelletsen i en argonatmosfär, sedan mäts viktminskningen och temperaturprofilen av pelleten medan den reduceras i en vätgasatmosfär, slutligen mäts temperaturprofilen av den reducerade pelleten i en argonatmosfär. Viktminskningen under reduktionen används för att beräkna reduktionsgraden under reduktionsförloppet.

Resultaten visade att reduktionshastigheten ökade med ökande temperatur och koncentration av H_2. Ökad temperatur gav även den största temperaturminskningen inne i pelleten då den reducerats med vätgas. Vid 900 °C uppmätes en temperaturminskning på 39 °C, varav reduktion vid 600 °C gav en temperaturminskning på 3 °C. Resultaten visar att efter en viss tids reduktion, spelar gasdiffusionen och värmeledningen genom produktlagret en viktig roll och är det som begränsar reduktions-hastigheten. Fortsatt, då hematitpelleten reducerades uppstod en platå där temperaturen var konstant och reaktionen till största delen var begränsad av värmeledningen genom produktlagret.

TABLE OF CONTENTS

1 INTRODUCTION

Greenhouse gases released into the atmosphere are causing warming of the environment, and by far the largest contributor is the carbon dioxide released through the burning of coal, oil and natural gas. These fossil fuels are burned to generate heat, electricity and power for industrial processes and transport respectively. To minimize the risk of devastating consequences of our climate system, it is necessary to limit the rise in the global average temperature well below 2 °C, preferably under 1.5 °C. Yet, greenhouse gas emissions keep increasing at a steady rate. Hence, the only way to reach the goal is to drastically cut back on the global greenhouse gas emission and later this century making them go down to zero. The Sweden Parliament has therefore decided to strive for a zero-net emission no later than 2045. [1]

Today the iron and steel production by itself stand for 10% of the CO_2 emission in Sweden and represent 7% of the total global CO_2 emission. In 2045 Sweden hopes to reach the national target goal of a zero-net emission of carbon dioxide. Ever since the process of the electric arc furnace (EAF) was brought to commercial usage, a lot of work has been put in to further improve the process. However, the prognosis of steel demand tells us that the scrap-based steelmaking will not be enough, hence ore-based steel production will play a significant role in the future. The reaction occurring during the reduction of iron oxides in a blast furnace (BF) represents about 85-90% of the total amount of carbon dioxide emission in ore-based steel production. [2]

In Sweden, the production of crude iron with today's technologies, i.e. the LKAB-SSAB production system, gives an emission of 1.6-1.7 tons of CO_2 per ton crude steel. Whereas the emission from a typical integrated steel plant in Western Europe is about 2.0-2.1 tons of CO_2 per ton of crude iron [3], thus, Sweden is one of the leading countries regarding producing steel in an efficient manner. However, it emits about 6 million tons of CO_2 per year, hence, developing a more sustainable route of iron production is necessary, and doing so before 2045 will contribute significantly to the target of a fossil-free Sweden. [2]

The Hydrogen Breakthrough Ironmaking Technology (HYBRIT) initiative will reduce iron ore pellets in similar shaft furnaces used in other parts of the world today, MIDREX or HYL processes. The main reductant, hydrogen, will only leave water and no carbon dioxide. The direct reduced iron (DRI) remains in its solid form and needs to be melted in an EAF before steel is produced. This will lead to a drastic increase in energy consumption, in the order of 15 TWh; this to melt the sponge iron and produce hydrogen through electrolysis. The largest cutback of carbon dioxide will be associated with the replacement of a BF by hydrogen-direct reduction plants (DR plants) and EAFs, i.e. the HYBRIT production principle. [2]

However, the implementation of this process is not straight forward and several problems need to be solved before a functioning process exists to produce steel in a fossil-free manner. As the reduction of hematite into sponge iron through hydrogen reduction is endothermic, a problem is that the temperature decrease, i.e. the temperature profile, inside the pellet during reduction is unknown. To be able to further understand and model the behavior of a hematite pellet during hydrogen reduction, the temperature profile during hydrogen reduction at 600 °C, 700 °C, 800 °C and 900 °C is investigated.

To be able to measure the temperature decrease inside the hematite pellet during hydrogen reduction, a small thermocouple that could be inserted into the center of the pellet was produced. The measurement was performed for six pellets, at four different reduction temperatures. This paper presents the results and the magnitude of temperature decrease in a hematite pellet during hydrogen reduction.

1.1 AIM AND SCOPE OF THE PRESENT THESIS

At DR-plants today, natural gas or syngas is used to reduce iron ore pellets into porous sponge iron. This process generates heat as the pellet is reduced. However, simple calculations show that by changing the natural gas into hydrogen, energy is consumed during the reduction process [4], [5]. The difference between the enthalpies for reducing Fe_2O_3 into sponge iron with CO(g) and H_2(g), calculated per mole iron, is equal to +23.1 kJ/mole Fe. Consequently, if one were to change from a CO-reduction method to an H_2-reduction method, 23.1 kJ/mole Fe amount of energy needs to be added to the system for the iron ore to be reduced.

Previous studies have proven that the reduction rate is strongly temperature-dependent [6]. Based on the calculated energy requirement, the temperature at the center of the pellet should not be the same as the temperature at the surface of the pellet but instead, decrease as the reduction reaction takes place. Hence, knowing the temperature difference between the inside and outside of the pellet is essential to estimate the rate of reaction, and other important properties of the reduced pellet.

The present work aims to record the temperature profile inside a hematite pellet while it is being reduced by hydrogen gas. Ideally, the results can be implemented in a model to better simulate the reduction reaction taking place inside a hematite pellet.

This report is limited to the examination of the KPRS pellets from LKAB. Experiments are restricted to measuring the temperature at the surface and the center of one pellet; hence, the thermocouples are fixated at these positions. Moreover, the thermocouples are fabricated in the lab and the accuracy of the readings is limited by experimental uncertainties. During the experiments, only one pellet is examined at the time, and the results are limited to measure the temperature effect inside one pellet. If a whole reactor is filled with pellets, the results from this study can only give a prediction on how the temperature profile and reduction curve should look and not give an absolute answer.

In the modern society we live in today, it is of high interest to develop new methods and models to improve and secure the life of future generations. Important aspects to consider when developing these new projects are the social, ethical, economic and environmental impact. This thesis investigates the temperature profile inside a hematite pellet during hydrogen reduction, to learn and understand the reduction process to be able to model the behavior inside a shaft furnace. No individual investigation of the social, ethical, economic or environmental effects has been carried out during this thesis work. But the HYBRIT initiative aims to meet the overall demand for steel in the next few decades by producing steel using the ore-based route and at the same time reduce the CO_2 emission. There are many factors affecting the cost of implementing the HYBRIT route, i.e. the price of coking coal, electricity and emission allowances. Therefore, being able to understand and model the behavior of the pellet during reduction is of high importance to be able to introduce the process in an optimized way. All of these important aspects will be more closely studied in further works.

2 BACKGROUND

2.1 PREVIOUS STUDIES

Globally, the hydrogen steelmaking route based on this new process is technically and environmentally attractive [6]. Xu and Cang are positive that by developing and applying *"CO_2 breakthrough technologies"* for steel and iron production, as well as using renewable energy sources, the CO_2 emission will be reduced in the long-run [3]. When reducing iron oxides with H_2, it is expected to yield iron with very low carbon content and hence be able to go directly to the secondary refining step, skipping the converting step, thus there is no need to remove large quantities of carbon. Moreover, Sohn H. Y. predicts that the reduced iron oxides will have a lower P and S content than the hot metal produced in the BF [7]. The following section will include a brief review of the most relevant studies on the subject, hydrogen reduction processes.

The kinetics and mechanisms of DRI production have been of interest for over half a century. Several authors have used thermogravimetric analysis (TGA) to investigate the reduction kinetics of iron oxides using different reduction gases [4]- [8]. The studies have shown that DRI contributes to higher efficiency in both BFs and EAFs, as well as it reduces the costs [9]. It is recognized that the rate-determining step in a reduction procedure is controlled by either the diffusion rate or chemical reaction rate, depending on the experimental conditions and properties of the metal oxide. For example, M. Kazemi et al. found that the reduction of iron oxide pellets by H_2 can be controlled by the chemical reaction and diffusion in the solid at the same time [10]. Furthermore, they found that by using H_2 as reducing gas, since it has a higher diffusion rate and faster chemical reaction rate, a larger overall reduction rate could be reached [11].

Ranzani da Costa et. al developed a mathematical model to simulate a DR shaft furnace operated with pure H_2 in order to evaluate the process. They concluded that DRI could be produced in a more compact reactor than the current MIDREX and HYL processes if pure H_2 gas was used. Moreover, this confirms the fact that reduction by H_2 is faster than that by CO. They also observed that pellet size and temperature of the inlet gas had a strong influence on the reduction rate: the smaller the pellet diameter, the faster the reduction and thus the more compact the reactor [6]. R. Beheshti et al. have reported properties that further affect the reduction rate. Those properties are the contact between the reacting phases, particle size and shape, the particle size distribution, the porosity and the pore distribution, the crystal structure and the gangue content distribution. [12]

The reaction rate decrease with the progress of reduction. Turkdogan et al. saw a diffuse iron/wüstite interface. This indicates that there is sufficient H_2 gas diffusion in the wüstite layer that some internal reduction takes place before the interface has caught up with the reaction front. The spread between the internal reduction and reaction front increases with; the progress of reduction, decreasing temperature and increasing porosity of the oxide (wüstite) [13]. Since many factors are affecting the reaction rate and mechanism of the reaction, care needs to be taken when the experimental condition is set, and the experiments are performed. Nonetheless, it is important to consider when a model is being developed.

Many different studies have been performed, but few of them have investigated the hematite pellet during hydrogen reduction. Often a composite or magnetite pellet is studied and reduced using different combinations of reducing gases. The following papers and publications include some of these setups, but also experimental procedures that are similar to the one used in this study.

S.K. Dutta et al. studied the non-isothermal reduction of iron ore-coal/char composite pellets. They performed non-isothermal measurements where they used two thermocouples, one above and one inserted into the core of the pellet. They expected that there would be a temperature gradient due to limitations in heat transfer during heating and due to endothermic reaction as well as temperature gradient along the furnace length. They observed temperature differences of 20-30 K, as well as they concluded that the reduction of iron oxides by H_2 become significant only above 850 K [14]. Cypres and Doudan-Moinet reported that hydrogen plays an important part in the reduction of iron oxides below 1073K [15], [16].

Hara et al. performed reduction experiments on iron oxide rods and pellets and measured the intraparticle temperature. They ran two experiments; one to know the reaction rate and the other to record the intraparticle temperature. The experiments showed that the temperature drop was larger at higher temperatures. [17]

The authors of "*Pressure Increase and Temperature Fall within a Hematite Sphere during reduction by Hydrogen*" showed that the pressure effect was governed by the rate of gas diffusion through the product layer. They measured an increased pressure inside the iron oxide sphere, as well as a temperature fall, during the reduction of an oxide pellet with hydrogen. However, the temperature difference was not so large, hence when they calculated the reaction rates for the isothermal and non-isothermal conditions, they gained similar results. [18]

Strangwa, Toppi and Ross carried out a study where they embedded a thermocouple inside hematite-magnetite briquettes and found that the reaction rate of magnetite to wüstite was larger than the one for wüstite to iron, both interfaces advanced linearly over time. The wüstite distribution remained constant after the incubation period, indicating that the last transformation is the most time-consuming step. The reduction of magnetite made the briquette crack and hence the results were not very reproducible. However, they proved both through thermodynamic calculations as well as experiments, that the temperature deviation is larger when reducing a magnetite briquette than a hematite one, i.e. -24 °C and -21.7 °C respectively. [5]

Y. Man et al. performed isothermal studies on iron ore-coal composite pellets and found that the reduction reaction, using solid coal as reductant, was not strictly topochemical, i.e. $Fe_2O_3 \rightarrow Fe_3O_4 \rightarrow FeO \rightarrow Fe$. The coal-based direct reduction process reduces iron ore into pure iron through solid-state diffusion [19]. Y. Man et al. ran more experiments, but this time introduced reducing gases such as hydrogen and carbon monoxide. Through X-ray diffraction (XRD) they found that the FeO mass percentage decreased rapidly in an H_2 atmosphere at 900 °C and that the rate of reaction was significantly more rapid in the H_2 atmosphere. In the scanning electron microscope (SEM) analysis of the samples, it could be found that the microscopic structure of the iron precipitation differed widely in CO and H_2 atmosphere at 1100 °C. The iron had a more porous appearance being reduced in the H_2 atmosphere, which could be the reason for the increased reduction rate [20].

At high temperatures, above 1400 °C, a dense iron layer is formed instead of a porous layer, which keeps the reduction rate approximately at the same rate as for reduction at 1300 °C [7]. Turkdogan et al. found that the pore structure became progressively coarser with increasing reduction temperature, 600-1200 °C. Moreover, they found that fine pores were present within the grains, which increase the effective diffusivity of the gas through the pores [13]. High temperatures yield a product with lower porosity, due to aging, longer reaction time is needed [21].

Wagner et al. confirm that the reduction occurs successively through rather separate reduction steps. The X-ray spectra showed that hematite reduction into magnetite occurs before wüstite is detected, whereas the reduction of wüstite into iron begins before the total consumption of magnetite. The last transformation takes the longest time, which may depend on a slow-rate chemical reaction at the wüstite-iron interface. Wagner et al. confirm that a higher reduction temperature accelerates the reaction rate [22].

Stalhane and Malmberg and Edström [23] and Turkodogan and Vinters [13] concurs with this finding. In both studies, different types of samples were reduced, and they could examine how the morphology influenced the rate of reduction. The authors found that the reactivity was higher for samples consisting of coarser hematite particles than for a sample consisting of nano-powder. They found that the nano-powder sample became very dense, and they concluded that the gaseous diffusion is the rate-limiting step.

Sun and Lu found that, if the off-gases from the reacting system, with temperatures of 500-600 °C, were reused for pre-reduction of magnetite concentrate pellets, a higher degree of reduction could be reached at earlier time steps. The off-gas could remove up to 25% of the oxygen in the magnetite pellet and result in an earlier formation of metallic iron, which in turn increases the effective thermal conductivity in the pellet, through which heat is supplied. Moreover, Sun and Lu found that the rate of reduction is significantly increased with increasing effective thermal conductivity. Hence, the conduction is the dominant heat transfer mechanism, and increasing its value is most important. [24]

Beheshti et al. point out that the overall performance of the DR reactor is strongly dependent on the gas-solid interaction, in terms of heat and mass transfer. The reduction occurs simultaneously throughout the production. Beheshti et al. performed small-scale laboratory experiments, reducing hematite pellets in a reactor with H_2/CO gas mixtures. They found that the reduction rate increased with increasing H_2 content in the gas mixture, temperature and porosity, whereas it decreased with increasing size of the pellet [12]. Consistent results were produced by M. Kazemi et. al [10], [25], Takahashi et al. [8], Kawasaki et. al [23] and Turkdogan et. al [13]. Further, Kawasaki et al. found that the reduction rate with hydrogen gas is approximately 5 times faster than carbon monoxide. Moreover, complete reduction could be reached at lower temperatures with hydrogen as reducing gas [23].

The experiments carried out by Fortini et. al [26], Rao [27] and Sun and Lu [24] gave the result that the reduction of iron ore carbon composites, follows a series reaction; $Fe_2O_3 \rightarrow Fe_3O_4 \rightarrow FeO \rightarrow$ Fe, i.e. each reduction reaction goes to completion before the next is started. However, a number of different authors do not validate this hypothesis e.g. Tien and Turkdugan [28] and Donskoi and Mcelwain [29].

But, Fortini and Fruehan [26] points out that some previous authors have not made it clear if they have reported several iron phases present at the same time during the reduction of a composite, nor where these phases were found. But, Spitzer, Manning and Philbrook reported results with several coexisting iron phases, when they reduced large specimens of iron oxides using CO and H_2 reducing gases [30].

2.2 STATE OF THE ART REVIEW

In just a few years, the interest in developing the reduction process even further has exploded. New techniques that want to solve the environmental crisis have been developed, and three of them are the fluidized bed, a pellet consisting of iron and biomass and a suspension process. These techniques are shortly introduced in the following section but will not be further evaluated in this study.

Over the past years, studies developing fluidized bed DR have become more common [9], [31]. The high raw materials cost, i.e. lump and pellets, and the environmental effect of the ordinary DRI process and BF route have driven the development [32], [33]. The process involves charging untreated iron ore fines, which accounts for about 2/3 of the world's iron-ore production, into the process. Through experiments, it was found that the reaction rate was affected by both temperature and gas composition. Using H_2 gas made the reaction proceed faster than when CO gas was used [9]. Pang, Guo and Zhao found that a high content of H_2 reductant made it possible to reduce iron ore fines smaller than 1 mm at a temperature of 750 °C. However, higher temperature, i.e. 800 °C, was needed when the fines were larger than 1 mm. They further proved that a higher H_2O percentage in the gas mixture decreases the reaction rate. Because the equilibrium partial pressure of H_2 decreases with increasing content of H_2O in the gas mixture and minimizes the driving force of the reduction reaction. The amount of H_2O should be kept below 10% to have an efficient reduction [31]. Problems with the procedure are that the particles tend to stick together, causing the reduction process to stop [32].

Another development of the DRI process is that of making composite pellets consisting of biomass and iron ore. The biomass is a renewable energy source with low contents of harmful elements, such as S and P. Through experiments, Gao et al. found that iron ore-biomass composites had higher reducibility than pellets without biomass, reduced using H_2 gas since the biomass increased the porosity. No characteristic difference could be seen in the SEM images taken of the different pellets, with and without biomass, demonstrating that the biomass did not affect the quality of DRI products. The authors found that the reduction temperature had a significant effect on the reduction extent. The initial stage of reduction of an iron oxide pellet is controlled by both gas diffusion and chemical reaction, and the contact area is the key factor. However, the overall reaction rate is mainly controlled by the interfacial chemical reaction, whether introducing biomass or not. The reduction process obeys the gas-solid reaction model, and the rate-controlling step is the chemical reaction turning FeO→ Fe [4].

A relatively uncommon approach, a novel alternative, to reduce both the energy consumption and the environmental effects of the ordinary ironmaking technology, the BF route, was presented by Sohn in his report "*Suspension Hydrogen Reduction of Iron Ore concentrate*". The technology of suspension process eliminates the coke making and pelletization/sintering step, thus it reduces fine iron oxide concentrates, magnetite, in a preheated stream of pure hydrogen gas or syngas. This method of reducing iron oxide was developed to sufficiently produce reduced iron oxides, such that it is intensive enough to replace the BF/BOF route. Hence the author state that the technology of DRI, hot briquetted

iron (HBI) and iron carbide is not intensive enough to be able to replace the production of iron through the BF/BOF route. SEM analysis showed that the product became more porous as the reduction proceeded and that increasing reaction temperature, 900 °C to 1100 °C, lead to increased porosity. However, at even higher temperatures, 1400 °C, a dense iron layer was formed, decreasing the reaction rate. The experiments showed that the suspension hydrogen reduction technology is a feasible procedure to produce iron, hence the reduction takes only a few seconds. [7]

3 MATERIALS AND EXPERIMENTAL METHOD

In the following section, the experimental procedure carried out to reduce six hematite pellets at four different temperatures will be presented. This section includes a detailed description of the furnace setup and sample preparation, as well as the experimental procedures, calibration of the scale and a paragraph presenting the development and improvement of the experimental procedure.

3.1 FURNACE SETUP

The experiments were performed in the furnace setup illustrated in Figure 1.

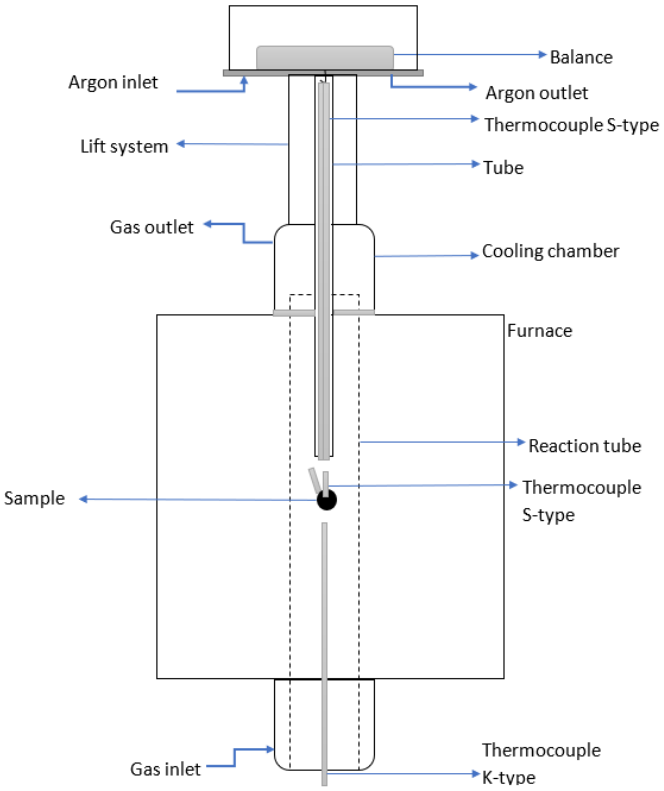

Figure 1, Schematic illustration of the experimental setup.

The setup consisted of a resistance furnace with a reaction tube made of fused silica, which was completely sealed by o-rings. A tube was connected to an aluminum plate, where a balance; Explorer® Precision electronic balance EX4202 from Ohaus, was placed and encapsulated by an acrylic glass lid. The precision balance with 0.001 g accuracy and high response speed was used and connected to a computer to record the weight of the samples. The tube was allowed to move vertically and inside two S-type thermocouples were hung in a hook underneath the balance. The thermocouples were connected to a computer and recorded the temperature change during the experimental execution. A basket made of Nikrothal was hung on the same rod as the thermocouples and a sample was placed in the basket. One of the S-type thermocouples was inserted into the center of the pellet and the other was placed such that it was in contact with the surface. The sample was placed in the cooling

chamber and sealed with o-rings. The cooling chamber was kept at temperatures of about 100-200 °C, and the pellet was placed there during heating and cooling of the furnace. An additional thermocouple of K-type was placed in the hot zone of the furnace, to make sure that the temperature inside the furnace was stable and reached the target temperatures. Inert argon gas and reactive hydrogen gas with purity 99.999% and 99.995% respectively, were used during all reduction tests.

3.2 SAMPLE PREPARATION

Pellets from LKAB, i.e. KPRS pellets (Kiruna Pellets Reduction Special), were used during the experiments. The pellets contained 96.88% hematite and a small number of other oxides, mainly SiO_2, CaO and MgO. The pellets had an average porosity and diameter of 26% and 1.2 cm, respectively. To protect the interest of the company, no detailed composition is provided.

The pellets with a diameter of 12 mm were prepared, given a hole in the center, using a diamond coated spiral drill. The hole had a diameter (1.2 mm) large enough to fit an S-type thermocouple and was deep enough for the thermocouple to reach the center of the pellet. A drill press with a velocity of 100 rpm, was used during this operation.

Two type-S thermocouples were prepared by welding a hot-junction between 10% rhodium/platinum and pure platinum wire. The wires were threaded through Al_2O_3 tubes with diameters of 4.2 mm and 1.1 mm, the larger tube hung from the scale, the smaller tube was inserted into the pellet.

3.3 DEVELOPING AND IMPROVING THE EXPERIMENTAL PROCEDURE

Three different setups of the type-S thermocouple were used. The setups can be seen in Figure 2, a) surface thermocouple measuring the temperature at a distance from the sample, b) surface thermocouple inside a 4.2 mm tube in close contact with the sample, c) surface thermocouple inside a 1.1 mm tube in close contact with the sample.

As the surface thermocouple was supposed to measure the temperature at the surface of the pellet, the first setup needed to be improved. The second setup was expected to solve the problem, with the thermocouple now touching the sample surface. However, it was found to measure the temperature profile of the 4.2 mm tube instead of the pellet temperature. And therefore the 4.2 mm tube was replaced by a much smaller tube, 1.1 mm, i.e. the same size as the one used to measure the center temperature. Measures were taken to perfect the method, the last setup was found to show the most stable results, and therefore only the results from the last setup will be discussed.

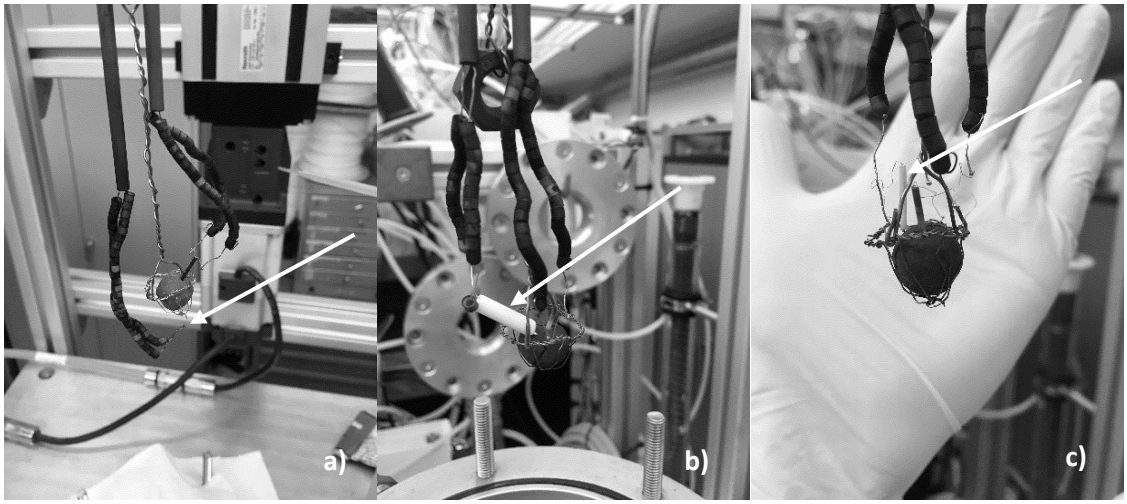

Figure 2, Different setups of the S-type thermocouples. a) first setup, no protective tube, b) second setup, 4.2 mm tube, c) third setup, 1.1 mm tube.

3.4 EXPERIMENTAL PROCEDURE

3.4.1 Measuring the temperature profile in a Fe_2O_3 pellet during H_2 reduction, new setup

The following procedure was used for every run, except for one, which will be presented in the next paragraph. This setup is used to evaluate the early stages of reduction.

A pellet was placed in a holder that was attached to a balance. A thermocouple of type-S was inserted into the center of the pellet, whereas another was positioned at the surface. The gas inlets allowed argon gas to enter the chamber both from the bottom and the top. The bottom gas inlet was used for introducing both the inert and reactive gas, whereas the top gas inlet, located inside the acrylic glass box which contained the balance, only allowed argon gas. A low flow rate of 0.01 L/min of argon gas was constantly flowing through the box of the balance during the temperature and sample weight recordings, to make sure that the balance did not encounter any hydrogen gas. All gas flow rates were controlled by Bronkhorst el-flow® select mass flow meters. Each experiment started when the furnace was carefully sealed and a flow rate of 2 L/min and 1 L/min of argon gas was passed through the system from the bottom and top gas inlet respectively, to drive away air.

Each experiment was composed of three sub-experiments. First measuring the temperature profile at the surface and center of the unreduced pellet, composing of hematite. Secondly, measure the temperature profile and mass loss during hydrogen reduction, at different temperatures. Lastly, measuring the temperature profile at the surface and center of the reduced pellet, composed of pure iron and some retained oxides. The argon atmosphere was maintained during both the heating and cooling of the pellet. During heating, the sample was retained in the water-cooled chamber. Heating and cooling rates of the furnace were set to 15 °C/min. After reduction, pictures of every pellet were taken to document the effects of the hydrogen reduction process.

To start, a total flow rate of 3 L/min of argon gas was kept during heating of the furnace, and after reaching the target temperature, the flow rates were reduced to 0.3 L/min at the bottom gas inlet and 0.01 L/min at the top gas inlet. During heating, the sample was retained in the water-cooled chamber. The flow rates were kept for 20 min after the target temperature was reached, to let the system reach a steady-state.

After the system had reached a steady-state, the sample was rapidly lowered to the hot zone of the furnace, in less than 10 s, using the lift system. The temperature on the surface ($T_{surface}$) and center (T_{center}) was constantly measured and recorded. After 20 min the sample was quenched by lifting it into the water-cooled chamber and flushing the system with argon gas with a total flow of 3 L/min. The flow rates of argon gas were kept for 20 min to let the sample cool down.

Thereafter, the argon gas entering the reaction chamber in the bottom gas inlet was replaced by hydrogen gas with a flow rate of 2 L/min, and the argon gas flow into the box of the balance was reduced to 0.01 L/min. The hydrogen gas was flowing through the furnace for 40 min and was then reduced to a flow rate of 0.8 L/min to homogenize and reach a steady-state. After 20 min, the sample was rapidly lowered into the hot zone of the furnace and temperature and sample weight were recorded. Each sample was quenched after different times of reduction, their times are tabulated in Table 1.

Table 1, The temperature and reduction time for each run.

Temperature	**600 °C**	**700 °C**	**800 °C**	**900 °C test A & B**	**900 °C test C**
Time	60 min	60 min	40min	25 min	130 min

A total flow rate of 3 L/min of argon gas was kept for 40 min to drive out the hydrogen gas from the furnace. The flow rates were then reduced to 0.3 L/min and 0.01 L/min for the bottom and top gas inlet respectively. The flow rates were kept for 20 minutes, to let the system reach a steady-state before the sample was rapidly lowered into the hot zone of the furnace. The temperature was constantly measured and recorded. After 20 min the sample was quenched, through the same procedure described above. The argon atmosphere was maintained during both the heating and cooling of the pellet.

3.4.2 Measuring the temperature profile in a Fe_2O_3 pellet during H_2 reduction, ordinary TGA setup

The following procedure was used in one run, where hydrogen gas was introduced to the furnace when the pellet had been placed in the hot zone, where the temperature was 900 °C. This experimental setup represents the ordinary thermogravimetric analysis (TGA) setup. This setup was used to compare the results from the previous runs at 900 °C.

The loading, sealing and heating of the furnace were carried out in the same way as described earlier. When the furnace had reached the target temperature, the argon gas flow rate was reduced to 0.3 L/min for the bottom gas inlet and 0.01 L/min for the top gas inlet, to let the furnace homogenize and reach a steady-state before the first measurement was carried out. After 20 min the pellet was lowered into the hot zone of the furnace, where the temperature was measured and recorded. After another 20 min, the pellet was not quenched but instead kept in the hot zone and hydrogen gas with a flow rate of 0.8 L/min was introduced into the furnace.

The pellet was reduced for a total time of 130 min, during which both the temperature and mass loss was recorded and was thereafter quickly retracted to the cooling chamber and quenched with a total flow rate of argon gas of 3 L/min. The flow rates of 2 L/min and 1 L/min for the bottom and top gas inlet respectively were kept for 40 min, removing the hydrogen from the furnace. After 40 min, the gas flow rate was reduced to 0.3 L/min and 0.01 L/min in the bottom and top gas inlet respectively and the furnace was let to reach a steady-state for 20 min.

At last, the pellet was lowered into the hot zone and kept there for 20 min. The temperature was constantly measured and recorded, thereafter it was quenched using the same procedure described above.

3.5 PRACTICALLY DETERMINED CORRECTION CURVE

It is known that the weight change indicated by a scale during TGA, seldom displays the true weight. The actual weight change occurring in a sample is hidden in the results, and only an apparent weight change is recorded [34]. To take this into account, experiments were carried out under identical conditions to those of the actual experiment, but this time an inert aluminum oxide pellet, Al_2O_3, was used. The inert pellet had approximately the same shape and volume as the examined pellets. When changing the gas in the furnace from argon to hydrogen gas, the buoyancy force was affected. This led to an apparent weight change of the inert pellet for each different temperature and experimental setup. Every setup recorded a weight change during the experiments, and the correction curves were used to correct the experimental data for each run.

4 RESULTS AND DISCUSSION

It was found that the temperature decrease was more prominent at higher temperatures than at lower temperatures. This was also found by Hara et al. [17]. The largest measured temperature difference was 39 °C, contradicting the results of K. Sato et al. [18] who reported no special effects of temperature difference. However, S.K. Dutta et al. [14] agreed to the results, hence they observed a temperature difference of 20-30 K in an iron ore-coal composite pellets during hydrogen reduction. The reason for this large temperature difference is because the reaction rate is much faster at high temperatures than at lower temperatures. Due to the temperature difference, the reaction rate constant at the surface had a 9 times larger value than the reaction rate constant at the center. The result reveals the importance of knowing the behaviors occurring inside a porous oxide pellet during reduction using H_2 gas.

4.1 TEMPERATURE PROFILES

Similar to this study, Hara et al. [17] performed reduction experiments on iron oxide rods and pellets and measured the intraparticle temperature. However, they ran two separate experiments, one to measure the intraparticle temperature and one to record the degree of reduction. In this study, only one pellet was used for each experiment to reach higher reliability of the method.

As stated in the experimental procedure, three recordings of the center temperature (T_{center}) and surface temperature ($T_{surface}$) were made for each pellet. The first recording was performed in argon gas, whereby the temperature profile inside an iron oxide pellet could be measured. The second temperature recording was made in an H_2 atmosphere, to see if the reduction reaction had any impact on the temperature profile. The last temperature recording was carried out in argon gas and measured the temperature profile inside a totally or partially reduced pellet. As for both temperature recordings in argon, they could potentially be used in future modeling work to calculate the effective thermal conductivity of the iron/wütite outer layer. Hereon after the different stages of experiments will be called *before reduction*, *during reduction* and *after reduction*.

There were three experiments carried out at the same temperature, i.e. 900 °C. Two of them were performed with the same procedure and were carried out to make sure that the method had good repeatability. These two experiments will be named *900 °C test A* and *900 °C test B* and report good repeatability. The comparison between the two runs is reported in Appendix 1. The other experiment was performed so that the pellet had a temperature of 900 °C when the gas switching took place, H_2 was introduced, simulating the ordinary TGA setup. The results from this experiment will hereinafter be called *900 °C test C*.

For every experiment, six different temperature profiles were recorded. Namely, the temperature in the center and the surface before reduction, during reduction and after reduction. Figure 3 shows the temperature profiles at the center of the pellet at 900 °C for test A, for the three different stages of reduction.

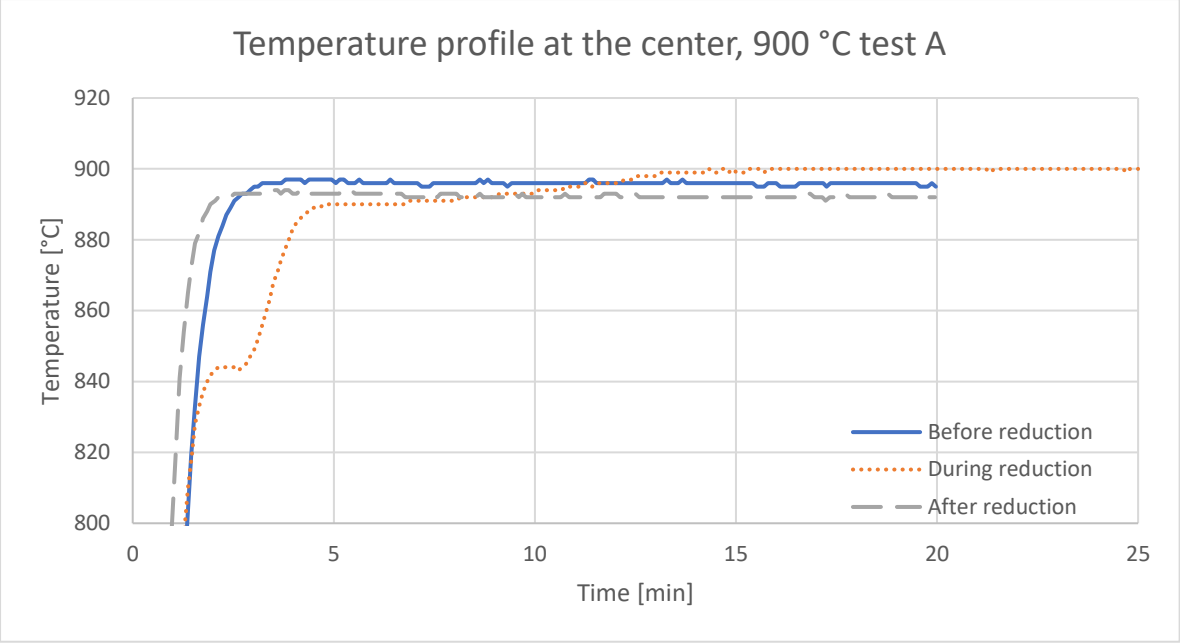

Figure 3, Measured temperature over time in the pellet center for test A at 900 °C, during the three phases of the experiment. The blue (solid) line and grey (dashed) line represent the temperature profile measured inside the pellet before and after reduction, respectively. The orange (dotted) line represent the temperature profile in the center of the pellet during reduction.

The graph shows that it takes about 3 min for the temperature in the center of the pure hematite pellet to reach the target temperature. Comparing it to the temperature profile in pure iron, after reduction, the time to reach the target temperature is shorter, about 2 min. Confirming that the effective thermal conductivity is higher in pure iron than in hematite. In Table 2, the time to reach the target temperature in the center of the pellet at different temperatures is presented.

Table 2, Time to reach target temperature in the center.

Temperature [°C]	Before reduction [min]	After reduction [min]
600	7	4
700	5	3
800	4	3
900 test A	3	2
900 test B	3	2
900 test C	3	1.5

Moreover, Figure 3 shows that the temperature profile in the center during reduction has a distinctive look and does not demonstrate the same behavior as the temperature profile curves before and after reduction. First, the temperature reaches a plateau value after 2 min, which it stays at until 2 min and 45 s. Then the temperature rapidly increases, before it reduces its rate again reaching its target temperature after about 14 min. In Table 3, the temperature and time at the plateau and the time to reach the target temperature is tabulated. It is shown that the temperature has a large effect on the plateau formation. The results show that the plateau lasts the shortest at 900 °C and the longest at

600 °C. The temperature at which the plateau arises differs a lot over the temperature range. At 900 °C, the plateau arose at 844 °C, and at 593 °C for the experiment carried out at 600 °C.

Table 3, The temperature, time at the plateau and time to reach the target temperature for each run.

Temperature [°C]	Plateau temperature [°C]	Time at the plateau [min]	Time to reach target temperature [min]
600	593	4.5 – 12	20
700	683	3.8 – 7.8	18
800	773	3 – 5.2	17
900, test A	844	2 – 2.8	14
900, test B	849	2.3 – 3.3	14

The plateau seen in the graph must be due to the reaction taking place. Calculating the standard enthalpy of reaction, one can compare the different energies between the carbon-based reduction route, Fe_2O_3 → Fe through CO (g) and hydrogen-based reduction route, Fe_2O_3→ Fe through H_2 (g). The enthalpy change is defined as the amount of heat absorbed or evolved during the following reactions, assuming that the temperature and pressure are constant:

$$^1/_3\, Fe_2O_3(s) + CO(g) = {}^2/_3\, Fe(s) + CO_2(g)$$

$$^1/_3\, Fe_2O_3(s) + H_2(g) = {}^2/_3\, Fe(s) + H_2O(g)$$

The enthalpy change is calculated for each reaction at a temperature of 900 °C [35].

$$Carbon - based\ reduction\ route, \qquad \Delta H: -10\,211 \left[{}^J/_{mol\ CO}\right]$$

$$Hydrogen - based\ reduction\ route, \qquad \Delta H: 24\,282 \left[{}^J/_{mol\ H_2}\right]$$

Comparing the different enthalpies of reaction, the carbon-based reduction is an exothermic reaction, whereas the hydrogen-based reduction is an endothermic reaction. The difference between the enthalpies calculated per mole iron is equal to + 23.1 kJ/mole Fe. So, if one were to go from a CO-reduction method to an H_2-reduction method, that amount of energy needs to be added to the system for the iron ore to be reduced.

The plateau occurs because the amount of energy required for the reaction to take place, heat consumption, is the exact amount of heat transferred to the reaction site. In Figure 3, the curve showing a plateau can easily be distinguished from the two curves measuring the temperature profile before and after reduction. The heat is transferred from the thermoelements in the furnace to the reaction site inside the pellet, through gas diffusion and conduction. As the pellet is being reduced a scale of iron oxide and pure iron is formed, shown by both Turkdogan et al. [13] and M. Kazemi et al.

[10]. The heat is conducted through a diffuse iron/wüstite layer until it reaches the reaction site. Wagner et al. [22] used X-ray spectra to characterize the phases during the reduction of hematite powder and saw that the hematite was completely reduced to magnetite before any wüstite was detected, and therefore it may be questionable how I choose to illustrate the partially reduced pellet, i.e. consisting of an unreacted hematite core. A schematic illustration of the pellet and its mechanisms of transferring heat can be seen in Figure 4.

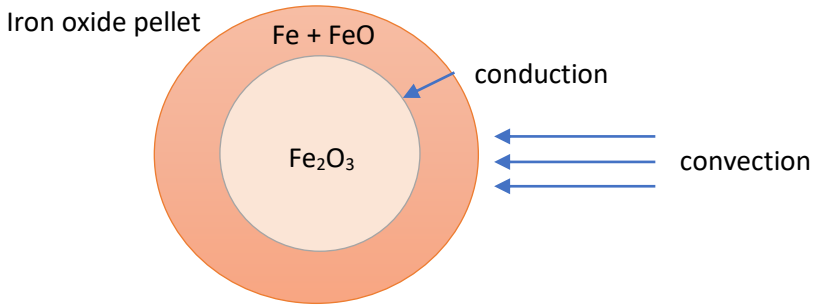

Figure 4, Schematic illustration of the pellet and its mechanisms of heat transfer in the system.

The reduction of a sintered pellet has been studied long before these experiments were carried out. Hence, it is well known that a gas-solid reaction of a solid particle, includes the following steps:

1. Mass transfer in the gas phase
2. Mass transfer through the product layer
3. The chemical reaction at the reaction interface

Since a mathematical model often becomes very complicated, it is common to focus on two or three steps of a process, which one thinks are the rate-limiting steps. For example, some researchers argue that the rate-controlling step is the mass transfer or the chemical reaction step, involved in the reduction of an iron oxide pellet [4], [13], [22], [23]. An effect that is often neglected is the:

4. Heat transfer through the product layer via conduction

From Figure 3, it is clear that the heat conduction through the forming scale is one of the rate-controlling steps during hydrogen reduction. Hence, a plateau is formed only during the reduction and is due to the chemical reaction taking place.

Secondly, from Figure 3 it can be seen that the center temperature during reduction reaches a higher temperature than it does in both runs in argon gas. This can be explained by the different thermal conductivity of hydrogen and argon gas. Because the hydrogen consists of smaller and lighter molecules, it has a larger thermal conductivity than the heavier and bigger argon molecules, hence, they can move faster and longer distances without colliding with an obstacle [36].

In Figure 5, the temperature profiles at the surface of the pellet for 900 °C test A, are plotted. The surface temperatures are recorded at the same time as the center temperatures which are displayed in Figure 3. The temperature measurement before and after reduction, follow the same trend and show only a small deviation of 5 °C. However, the temperature profile during reduction, show different

behavior. Its rate at which the temperature increases, slows down approximately at the same time as the temperature in the center decreases, initiating the formation of a plateau. The temperature decrease is due to heat conduction from the surface of the pellet to the reaction site, where the reduction reaction is taking place. The rate at which the temperature increases at the surface, decreases slightly before it reaches a steady-state after about 5 min.

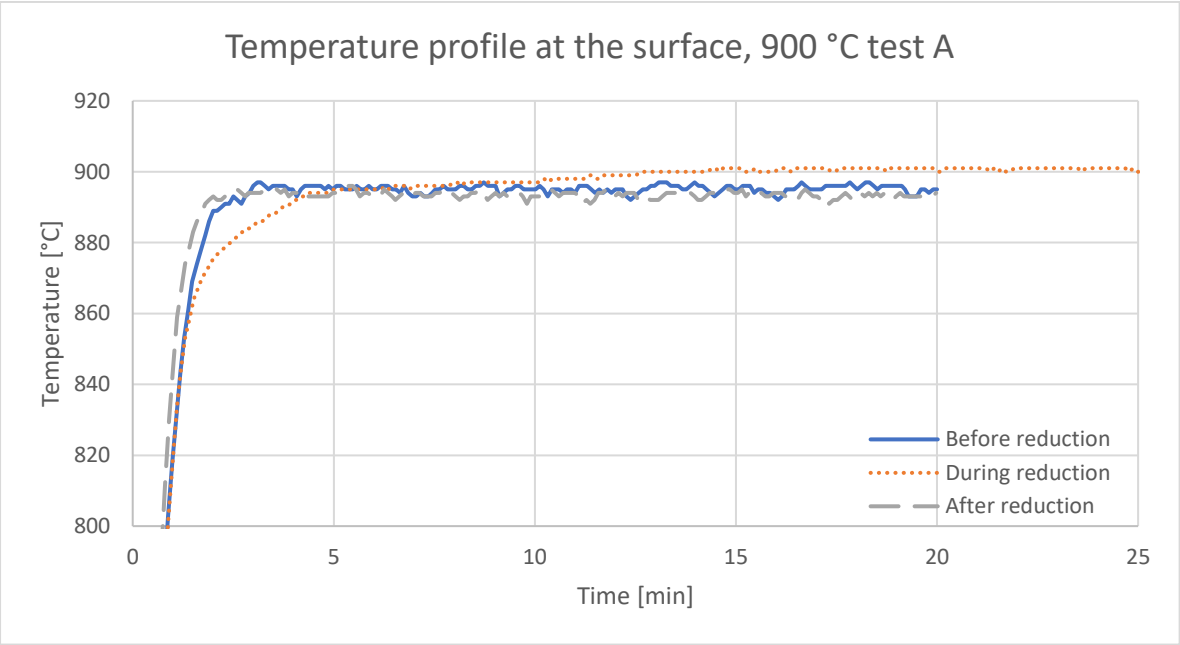

Figure 5, Measured temperature over time at the pellet surface for test A at 900 °C, during the three phases of the experiment. The blue (solid) line and grey (dashed) line represent the temperature profile measured at the surface of the pellet before and after reduction, respectively. The orange (dotted) line represent the temperature profile at the surface of the pellet during reduction.

4.1.1 Measuring the temperature profile in a Fe_2O_3 pellet during Ar_2 gas heating, before reduction

In Figure 6, the temperature profiles recorded inside and at the outside of the hematite pellets at different temperatures are displayed. The curves show the same behavior, independent of the furnace temperature, and therefore the run *900 °C test A* will represent the typical temperature profile and will be discussed further. The temperature profile for 900 °C test A before the reduction has taken place, is shown in Figure 7.

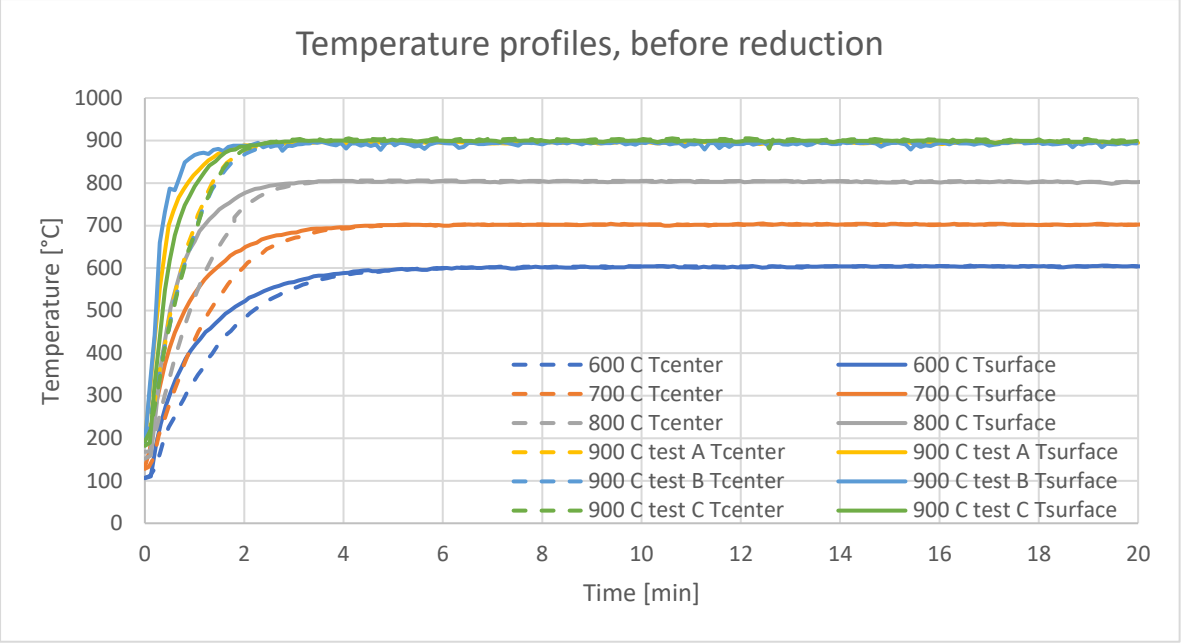

Figure 6, Measured temperature over time at pellet surface and center, before reduction, for furnace temperatures set to 600 °C, 700 °C, 800 °C and 900 °C. The solid and dashed lines represent the temperature at the surface and center, respectively.

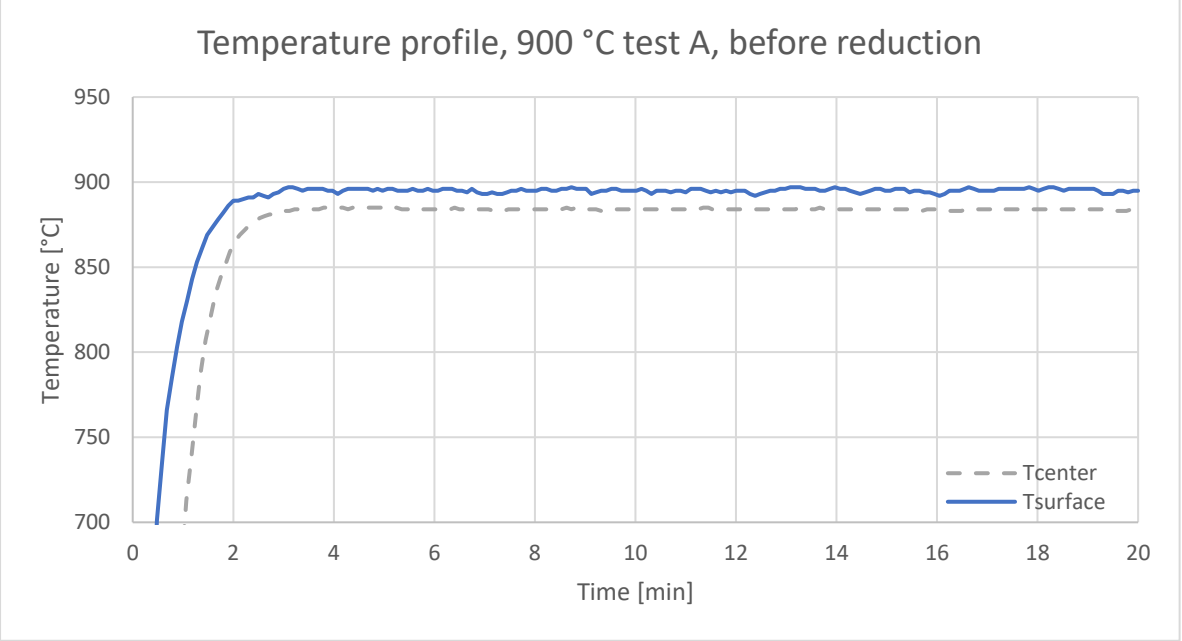

Figure 7, Measured temperature profile before reduction, 900 °C test A. The blue (solid) line and grey (dashed) line represent the temperature profile measured at the surface and center of the pellet, respectively.

The time to reach a steady-state temperature is faster for the measurement at the surface than the measurement in the center. Figure 7 shows that $T_{surface}$ reaches a steady temperature of about 30 s before T_{center}, and it is due to that the heat transfer through the porous hematite pellet takes some time.

Further, it is observed in Figure 7 that the temperatures in the center and at the surface, never reaches the same value. The deviation is about 11 °C and is due to experimental uncertainties, most likely due to the self-made thermocouples. The systematic errors are assumed to have a constant deviation from the true value and hence the T_{center} curve is normalized so that it reaches the same temperature as $T_{surface}$ at the end of each run. Figure 8 displays the normalized temperature profile at the center and surface, when the furnace temperature is set to 900 °C, test A. The normalized T_{center} curve reaches the same temperature as $T_{surface}$, i.e. the target temperature, after 3 min. Hereon after the temperature profiles will only include normalized temperature curves.

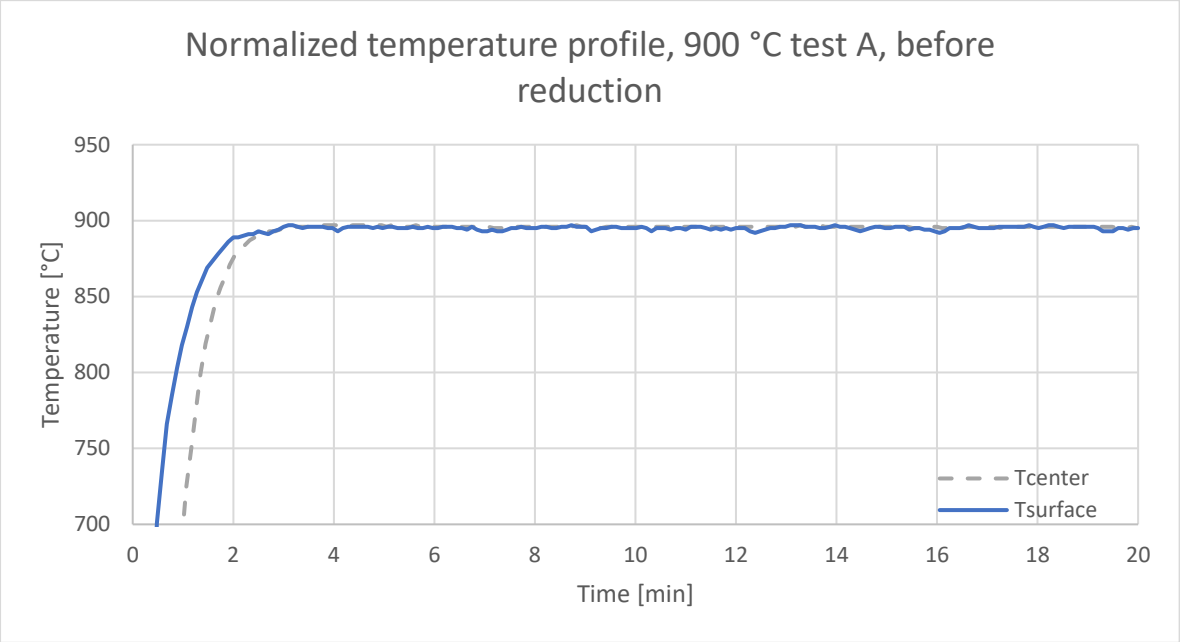

Figure 8, Normalized temperature profile before reduction, 900 °C test A. The blue (solid) line and grey (dashed) line represent the temperature profile measured at the surface and center of the pellet, respectively.

4.1.2 Measuring the temperature profile in a Fe_2O_3 pellet during H_2 reduction, new setup

In Figure 9 the temperature profile during H_2 reduction performed at 900 °C: *900 °C test A* and *900 °C test B*; are plotted. The grey lines show the results from the *900 °C test A* run, and the blue lines show the results from the *900 °C test B* run. The temperature in the center of the pellet reaches a plateau at 844 °C after 2 min and 849 °C after 2 min and 20 s for *900 °C test A* and *900 °C test B* respectively.

As stated in the previous paragraph, the center temperature show a tendency of reaching a plateau value in all the runs, this tendency can be seen in Figure 10. However, the center temperature for all the runs but *900 °C test A* and *900 °C test B*, show a slight decrease at the plateau stage. Figure 10 is used to illustrate the drop in temperature occurring during the reduction. From the Figure, it is clear

that the temperature widely affects the size of the temperature decrease. The decrease of T_{center} and $T_{surface}$ is due to the endothermic reaction taking place at the reaction site since the heat consumption is larger than the amount of heat transferred to the system. The temperature decrease at the plateau at different temperatures is tabulated in Table 4.

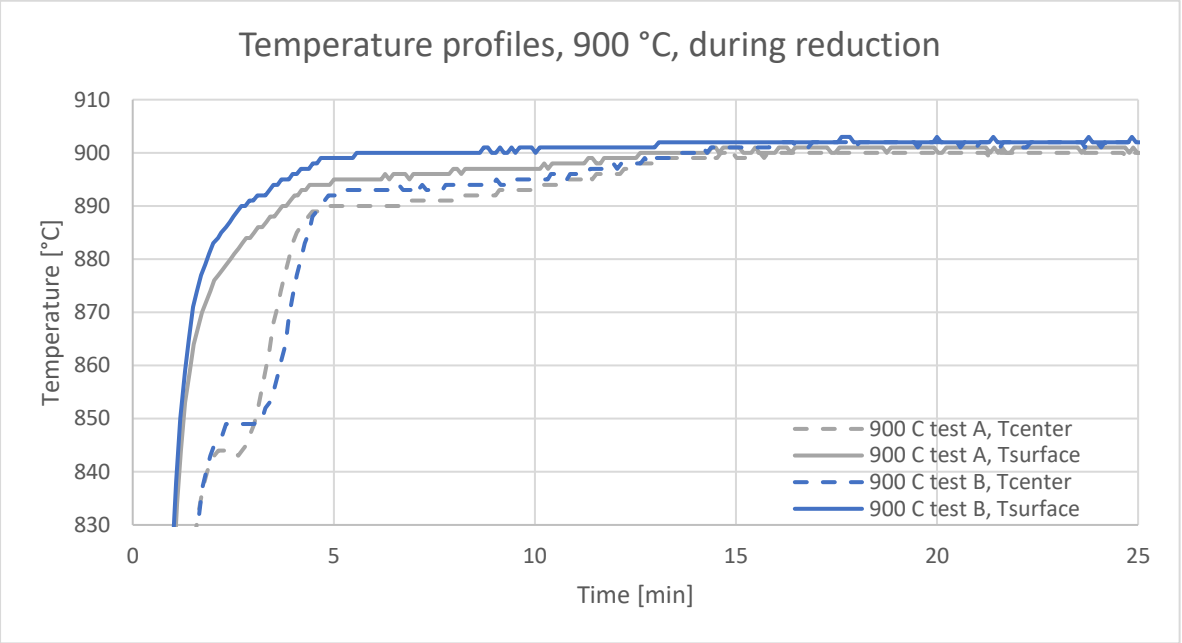

Figure 9, Measured temperature profiles during reduction at 900 °C. The blue lines represent the results from 900 °C test A, and the grey lines represent the results from 900 °C test B.

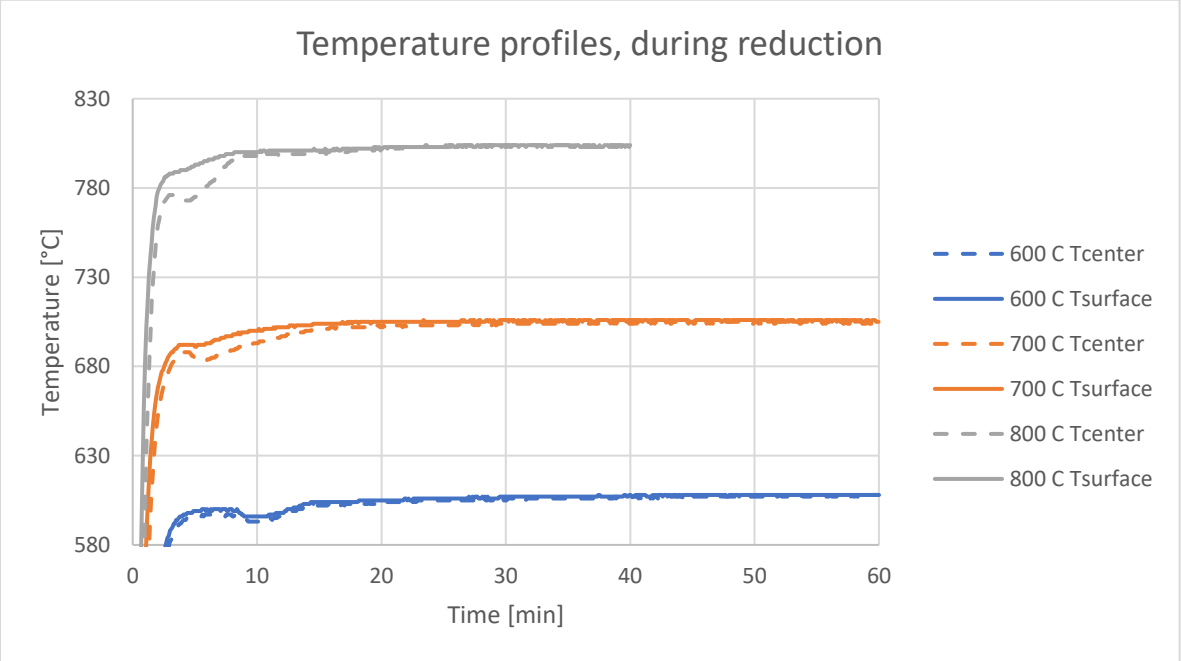

Figure 10, Measured temperature over time at pellet surface and center, during reduction, for furnace temperatures set to 600 °C, 700 °C, 800 °C. The solid and dashed lines represent the temperature at the surface and center, respectively. The blue, orange and grey lines represent the results from 600 °C, 700 °C and 800 °C respectively.

Table 4, Temperature decrease at the plateau due to endothermic reaction, different temperatures.

Temperature [°C]	Temperature decrease at the plateau [°C]
600	-4
700	-5
800	-3
900 test A	0
900 test B	0

4.1.3 Measuring the temperature profile in a Fe_2O_3 pellet during H_2 reduction, ordinary TGA setup

Because the experimental setup used in this study differs from the ordinary TGA setup, the results are presented separately. The following paragraph will include the result and discussion from the experiment simulating an ordinary TGA setup. Its result is presented in Figure 11, and it shows a large temperature drop when the hydrogen gas is introduced. The experiment was carried out for 130 min, to make sure that the atmosphere in the furnace had reached 100% H_2. The results showed that a reduction reaction started as soon as the hydrogen gas entered the furnace, hence, the graph display the first 30 minutes of reduction.

At time 0, the gas is switched from argon to hydrogen gas. From Figure 11, a small increase in temperature at the surface is noted. At this stage, the heat transfer is controlled by the mass transfer in the gas phase and the temperature increase is due to the higher thermal conductivity of hydrogen. After about 1 min, the center and surface temperature start to decrease. The heat conduction through the forming scale become more important and may be the controlling factor of the reaction rate. At time 4 min and 20 s, the temperature at the center and surface starts to increase again, with a high rate, to later reduce their rates again at 6 min. The drop in temperature occurs at 896-860 °C, between the time 1-6 min. Here a mixture of mechanisms control the reaction rate, the chemical reaction and the heat transfer through the forming layer. Thereafter, the center temperature increases at a slow rate, until it reaches the target temperature after 18 min. During this period, the reaction rate is controlled by the gas diffusion through the forming layer and the chemical reaction, a mixed-control mechanism. Table 5 reports the temperature at the center, the temperature decrease and time at the plateau, as well as the time to reach the target temperature.

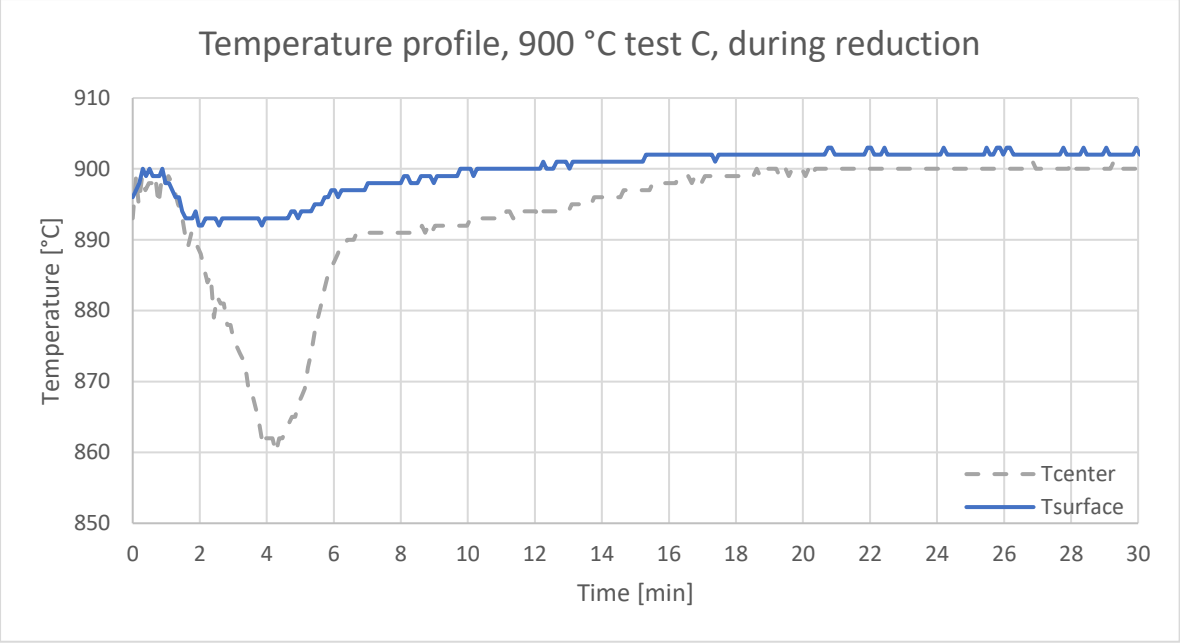

Figure 11, Measured temperature profile during reduction, 900 °C test C. The blue (solid) line and grey (dashed) line represent the temperature profile measured at the surface and center of the pellet, respectively.

Table 5, The temperature, temperature decrease, time at the plateau and time to reach the target temperature for 900 °C test C.

Temperature [°C]	**Plateau temperature [°C]**	**Temperature decrease at the plateau [°C]**	**Time at the plateau [min]**	**Time to reach target temperature [min]**
900, test C	896-860	-36	1 – 6	18

4.2 Degree of Reduction of a Fe_2O_3 pellet reduced in H_2

The degree of reduction is calculated by Eq. 1.

$$R = \frac{W_0 - W_t}{W_0 - W_\infty} \qquad \text{(Eq. 1)}$$

where W_0 is the initial weight of the pellet, W_t is the weight of the pellet at time t and W_∞ is the theoretical weight after complete reduction.

Figure 12 show the degree of reduction for each experiment using the correction curve, described in the method, to calibrate the scale. From the Figure it is noted that for some experiments, that the degree of reduction is reaching values greater than 1 (100%). This can never be the case since 100% reduction is the furthest a reduction reaction can proceed. Therefore, the degree of reduction curves will be normalized toward the estimated values marked with an "X" in Figure 12. These degrees of reductions are calculated using the initial and final weight of the samples. The normalized degree of

reduction curves are the measured weight loss curves (corrected with each correction curve), normalized to reach the final weight of the pellet. Figure 13 display the normalized degree of reduction curves at each temperature.

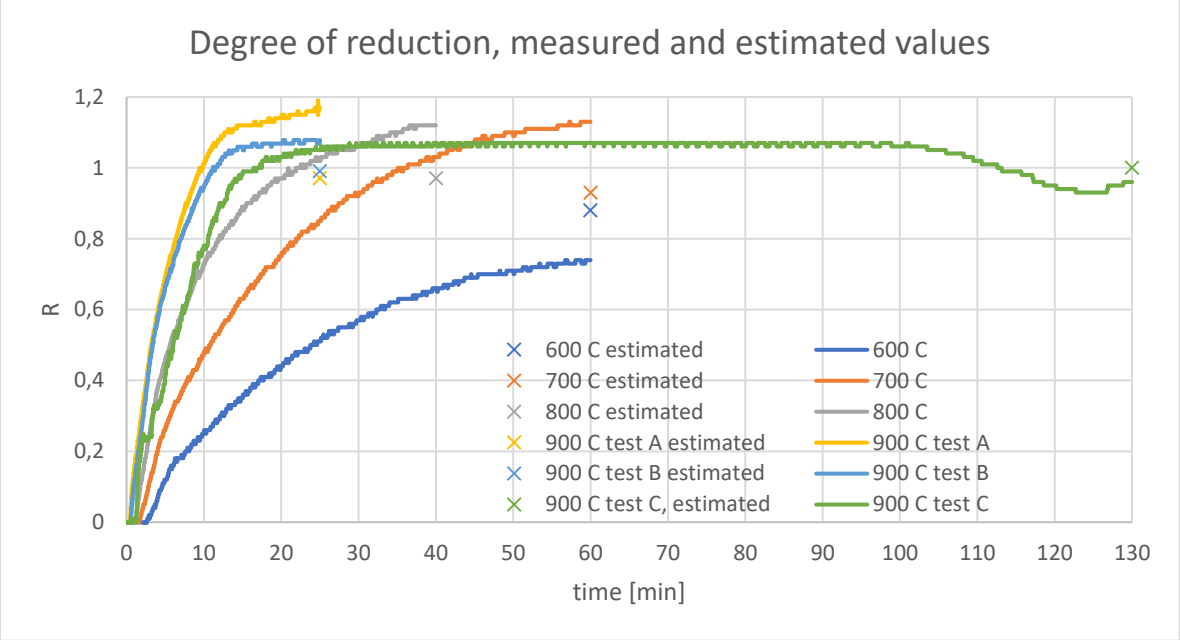

Figure 12, Measured and estimated degree of reduction curves. Where the curves are, from left to right; 900 °C test A (yellow), 900 °C test B (light blue), 900 °C test C (green), 800 °C (grey), 700 °C (orange) *and* 600 °C (dark blue).

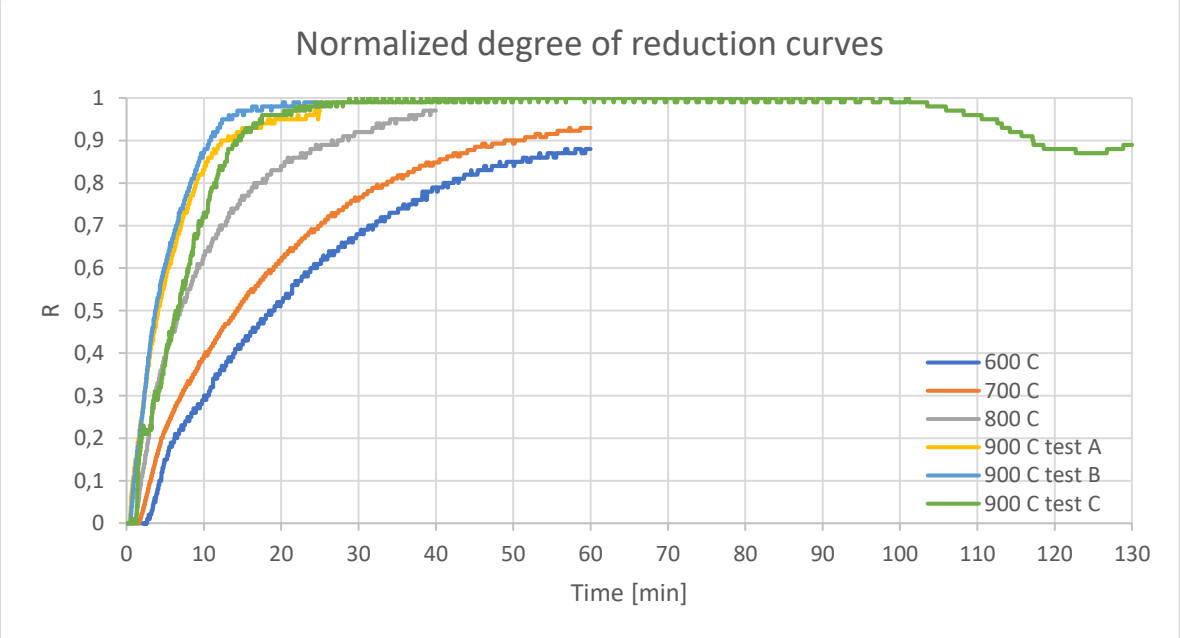

Figure 13, Degree of reduction, normalized curves at different temperatures. The curves from left to right; 900 °C test B (light blue), 900 °C test A (yellow), 900 °C test C (green), 800 °C (grey), 700 °C (orange) *and* 600 °C (dark blue).

The reduction rates increase with temperature, i.e. a longer holding time is needed for a pellet to reach a 100% reduction at *600 °C* compared to *900 °C*. The final degrees of reduction for each run are listed in Table 6.

Table 6, Final degree of reduction and time to reach its value.

Temperature [°C]	Time [min: s]	R
600	59: 18	0.88
700	58: 42	0.93
800	38: 24	0.97
900, test A	24: 18	0.97
900, test B	20: 12	0.99
900, test C	29: 41	1

Comparing the *900 °C test C* curve, with the *900 °C test A* curve, it is evident that the gas switching affects the reduction rate. The gas switching leads to a delay in reaction because the concentration of hydrogen is zero at the experiment start when the gas switching to hydrogen takes place. Figure 14 displays the degree of reduction during the first 20 min of these two experiments. The *900 °C test C* curve shows no reduction until about 1 min and 20 s of hydrogen flushing. At that time a sharp increase in the degree of reduction curve is measured, whereas it dulls off and reaches a plateau at 2 min. The degree of reduction gradually increases and becomes more stable after some time. After about 16 min, the two runs reach the same reduction extent, i.e. R=0.93.

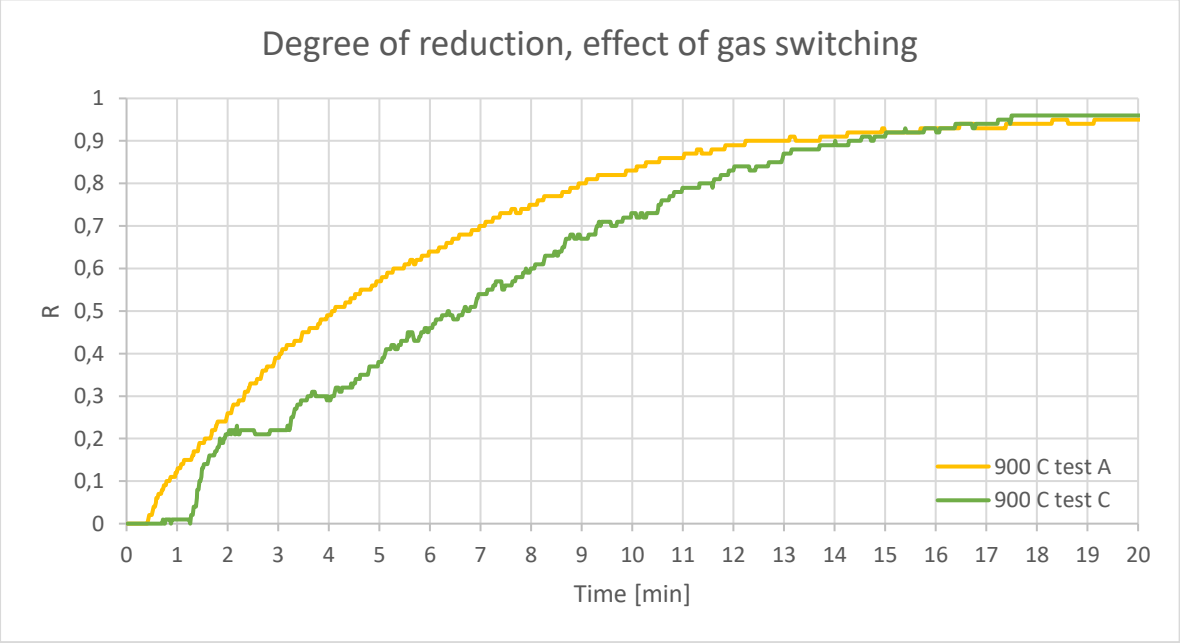

Figure 14, Degree of reduction at 900 °C, 900 °C test A and C, behavior due to gas switching.

Assuming the chemical reaction takes place as a 1st order reaction and the reduction process is controlled by the chemical reaction, mass transfer and heat transfer through the product layer, the total rate of reduction can be described by Eq. 2 and Eq. 3.

$$\frac{dR}{dt} = A\frac{P_{H_2} - P_{H_2,eq}^{RS}}{\alpha + \beta + \gamma} \quad \text{(Eq. 2)}$$

$$\frac{dR}{dt} = A\frac{T_{surface} - T_{interface}}{\delta} \quad \text{(Eq. 3)}$$

Where $\frac{dR}{dt}$ is the overall rate of reduction, A the is diffusion or surface area of the reaction interface, P_{H_2} is the partial pressure of H_2 in the gas stream, $P_{H_2,eq}^{RS}$ is the equilibrium pressure at the reaction site, $T_{interface}$ is the temperature at the reaction interface at time t, $T_{surface}$ is the temperature at the surface of the pellet, $\alpha, \beta, \gamma \; and \; \delta$ are the resistances due to mass transfer in the gas phase, mass transfer in the solid phase, chemical reaction and heat transfer through the solid phase, respectively. Where Eq. 2 describes the total rate of reduction due to concentration differences inside the pellet and Eq. 3 the total rate of reduction due to temperature differences inside the pellet.

From Eq. 2, it is clear that the reaction rate is proportional to the different pressures occurring in the gas stream and at the reaction site. When the gas switches from argon to hydrogen gas, the P_{H_2} in the initial stage is low, resulting in a low reaction rate. Not until 1 min and 20 s of hydrogen flushing with a flow rate of 0.8 L/min, the reaction takes place, explaining the behavior of the *900 °C test C* curve. Pang et al. also found that the partial pressure of hydrogen affected the reaction rate. In their study, they investigated how the water content affected the reaction rate [31].

4.2.1 Temperature effect on the degree of reduction of a Fe_2O_3 pellet

From Figure 9, Figure 10 and Figure 11 it is clear that the furnace temperature has a large effect on the temperature difference during the reduction process. The temperature differences, $T_{surface}$ - T_{center}, at the plateau are tabulated in Table 7. The results show that higher reduction temperatures cause a larger difference between the center and surface temperature. The temperature differences are greater at the higher reduction temperatures because the reaction rate is much faster at high temperatures than at lower ones.

Table 7, The temperature difference during reduction at different furnace temperatures.

Temperature [°C]	**Temperature difference, $T_{surface}$-T_{center} [°C]**
600	3
700	9
800	18
900, test A	38
900, test B	39
900, test C	33

From the Arrhenius equation, Eq. 4, it is evident that the temperature has a large effect on the reaction rates.

$$k = k_0 * e^{-\frac{Q}{RT}} \quad \text{(Eq. 4)}$$

Where k is the chemical rate constant, k_0 is the frequency factor constant, Q is the activation energy, R the universal gas constant and T the absolute temperature. Since the rate of temperature increase inside the pellet decreases as the reaction takes place, forming a plateau, it will affect k; the reaction rate constant, and also affect the total rate of reaction.

Figure 15 illustrates the degree of reaction and the temperature profile for the *900 °C test A* run. Looking at the degree of reduction curve, the apparent reaction rate is proportional to the slope of the curve. In Figure 15 the black curve shows that the apparent reaction rate at the plateau is higher, i.e. it has a steeper inclination, than the reaction rate after the plateau when the temperature rapidly increases. The reason for this can be explained by introducing a schematic illustration of the reduction behavior of the pellet. Schematic illustrations of the pellet at the beginning and after the plateau are presented in Figure 16. The shrinking unreacted core model is applied to illustrate the pellet's inside.

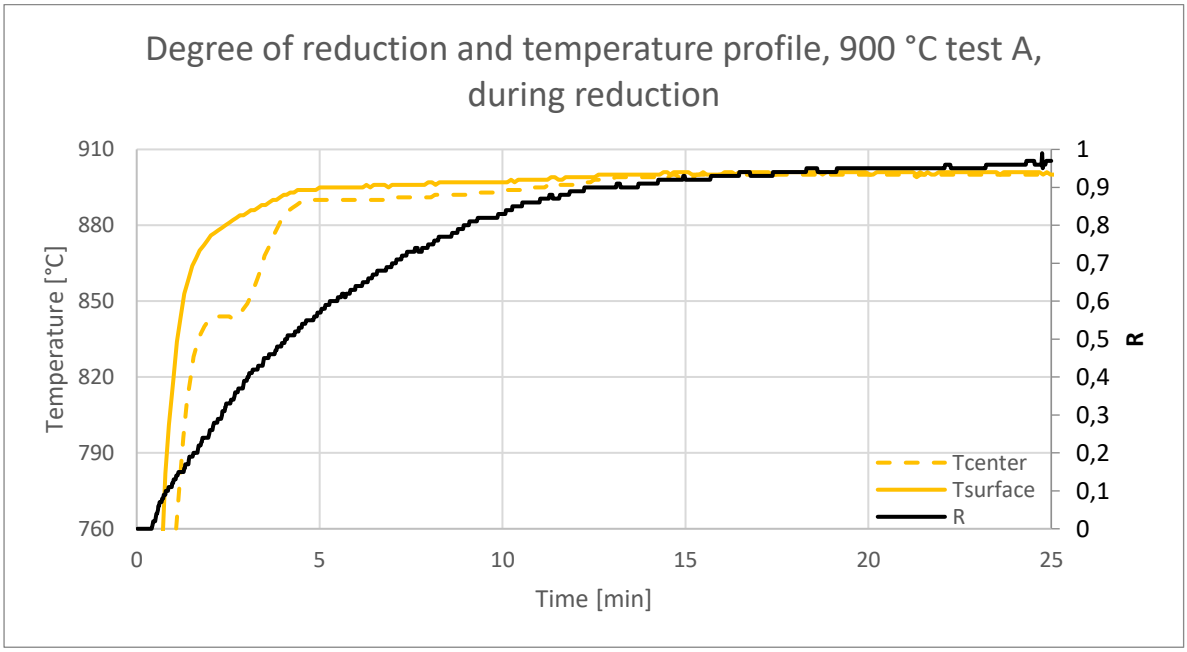

Figure 15, Temperature profile and reaction extent, the furnace is set to 900 °C.

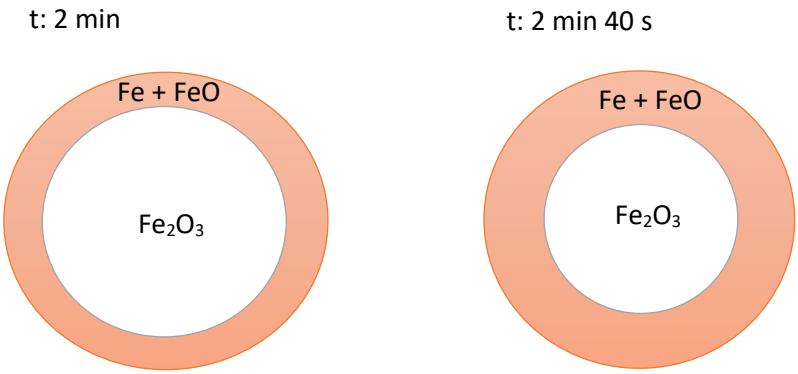

Figure 16, Schematic illustration of the pellet during reduction, R=0.26 and R=0.37.

To the left, an illustration of the pellet after 2 min of reduction, reaching R=0.26 is presented. At the right, the pellet has been reduced for 2 min and 40 s reaching R=0.37. At the beginning of the plateau, the pellet has reached 26% of reduction and the iron/wüstite outer layer is thin but has higher thermal conductivity than the unreacted core. Moreover, the surface area of reduction is large, and since the frequency factor constant, k_0, depends on the collision rate, the surface area will affect the reaction rate constant. This leads to:

- Large surface area of reaction: k_0= large
- Activation energy and temperature is constant: Q & T=constant
    - Reaction rate constant: k= large

After the plateau, at 2 min and 40 s, the iron/wüstite layer has increased its thickness and the reaction interface has decreased its size. At this stage, the transferred energy becomes greater than the consumed energy, thanks to the conduction through the iron/wüstite layer. The imbalance of heat consumed and transferred to the pellet's inside, gives an increase in temperature. This leads to:

- Smaller surface area of reaction: k_0=small
- Activation energy and temperature increases: Q & T=increases
    - Reaction rate constant: k=smaller

Through this reasoning, the apparent reaction rate constant at the plateau is larger than the apparent reaction rate constant after the plateau. Further on, to compare the reaction rate constants for the different runs, the Arrhenius equation, Eq. 4, is rewritten in the form of Eq. 5. The ratio between the reaction rate constants at the surface ($k_{surface}$) and the center (k_{center}) of the pellet can be calculated for each run of experiments.

The following assumptions are made:

1. Activation energy is equal to: 80 [kJ/mol]
2. The temperature at the center: T_{center} > 400 [°C]

$$Ratio = \frac{k_{surface}}{k_{center}} = \frac{e^{-\frac{Q}{RT_{surface}}}}{e^{-\frac{Q}{RT_{center}}}} \quad \text{(Eq. 5)}$$

The ratio calculations are tabulated in Table 8 and confirm that the reaction rate constant at which the reaction takes place is affected by the temperature difference inside the pellet. A large temperature difference between $T_{surface}$ and T_{center} leads to a large ratio, hence the reaction rate constant at high temperature, e.g. $T_{surface}$ 900 °C test A, is much larger than at the low temperature in the center, T_{center} 900 °C test A. In the *900 °C test A* run, the temperature difference results in a 9 times higher reaction rate constant at the surface of the pellet than in the center. The result reveals the importance of knowing the behaviors occurring inside a porous oxide pellet during reduction using hydrogen gas.

Table 8, Ratio between the apparent reaction rate constant at the surface and in the center of the pellet.

Temperature [°C]	**600**	**700**	**800**	**900, test A**	**900, test C**
Ratio	203%	372%	745%	908%	100%

As the temperature difference decreases, i.e. the pellet is reaching higher degrees of reduction, the reaction rate constants reach almost the same value and the ratio approaches 1. As stated previously the temperature have a large effect on the rate of reaction. At lower temperatures, the reaction rate constant is lower and hence the ratio between $k_{surface}$ and k_{center} becomes less profound, giving smaller ratios. The results tabulated in Table 8 indicate that the heat transfer through the product layer is necessary to understand and include in future process modeling work.

4.2.2 Degree of reduction vs temperature profiles

In Figure 17, the degree of reduction and temperature profile curves for *900 °C test A* are displayed. The degree of reduction reaches a value of 0.57 before the temperature inside the pellet approaches a steady-state. I.e. 57% of the pellet has been reduced, meanwhile, the temperature inside the pellet has been non-isothermal. Again, this proves the importance of knowing and understanding the temperature behavior inside a pellet during hydrogen reduction, thus most of the reduction takes place before the temperature in the center of the pellet reaches a steady-state.

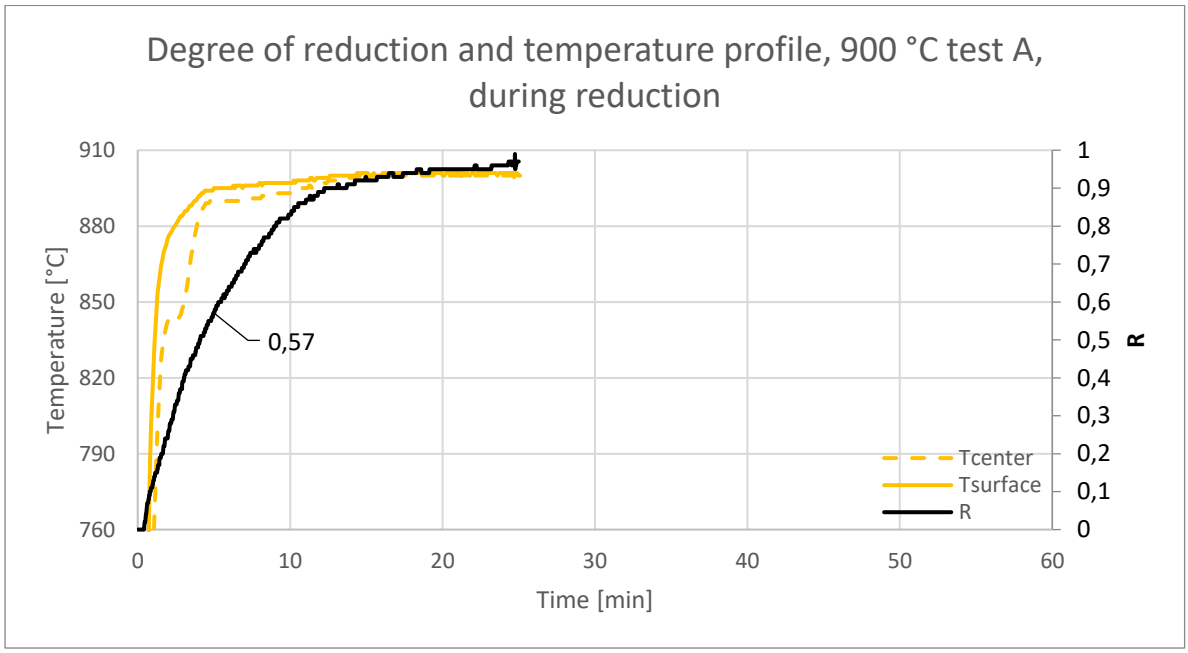

Figure 17, Comparison between the temperature profile during reduction and degree of reduction, 900 °C test A. The black curve represents the degree of reduction, whereas the colored curves display the temperature profile during reduction. The degree of reduction reaches a value of 0.57 before the temperature in the center reaches a steady-state.

Table 9 reports the degree of reduction for each temperature before the temperature in the center reaches a steady-state. At lower temperatures, e.g. 600 °C, the pellet reaches a smaller degree of reduction before the temperature in the center reaches a steady-state, whereas, at higher temperatures, a larger degree of reduction is reached. Again, this confirms that the rate of reaction is

faster at higher temperatures. Identical Figures including the temperature profiles and degree of reduction for each experiment are presented in the following section, Figure 18-Figure 22.

Table 9, The degree of reduction before the temperature in the center reaches a steady-state for each temperature.

Temperature [°C]	**600**	**700**	**800**	**900, test A**	**900, test B**	**900, test C**
R	0.41	0.55	0.55	0.57	0.61	0.54

At temperatures of 600 °C, the pellet reaches a degree of reduction of 0.41, before the temperature in the center reaches a steady-state. At 600 °C, the reaction rate curve has a gradual incline and reaches a maximal reduction degree of 0.88 after 60 min of reduction.

As the temperature increases, looking at the other experimental results in Figure 19-Figure 22, the curves take on a steep inclination and reach higher reduction degrees at shorter times. Higher temperatures give a larger degree of reduction and confirm that the rate of reduction is faster at higher temperatures. Again, this proves the importance of understanding the temperature behavior inside a pellet during hydrogen reduction.

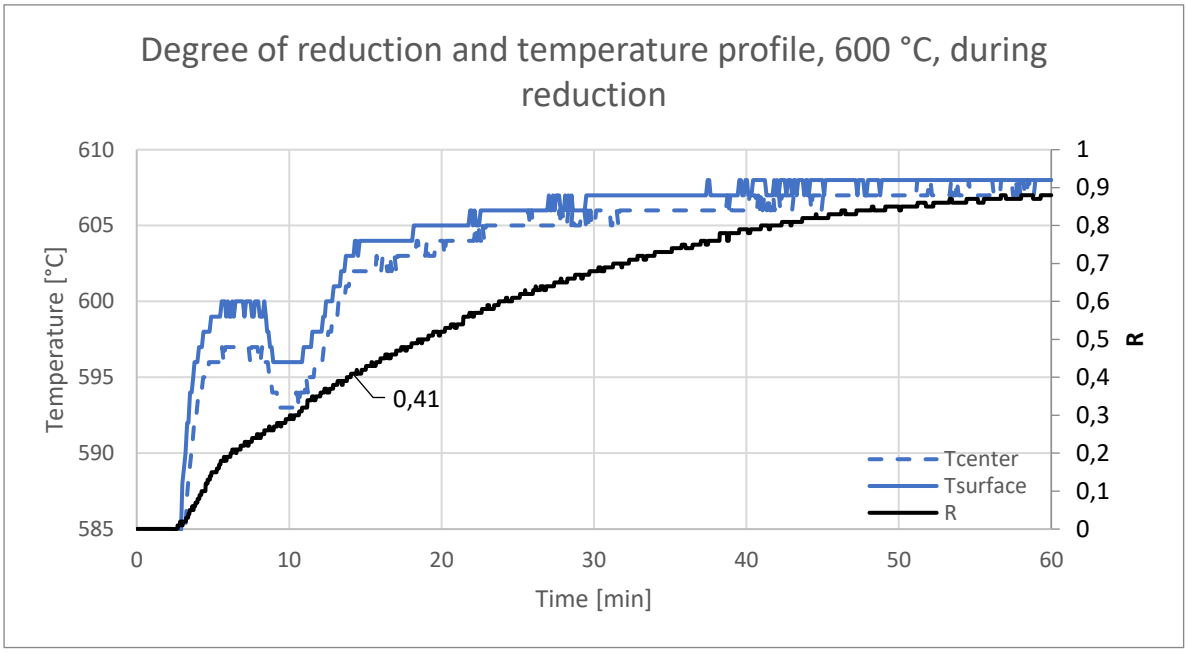

Figure 18, Comparison between the temperature profile during reduction and degree of reduction, 600 °C. The degree of reduction reaches a value of 0.41 before the temperature in the center reaches a steady-state.

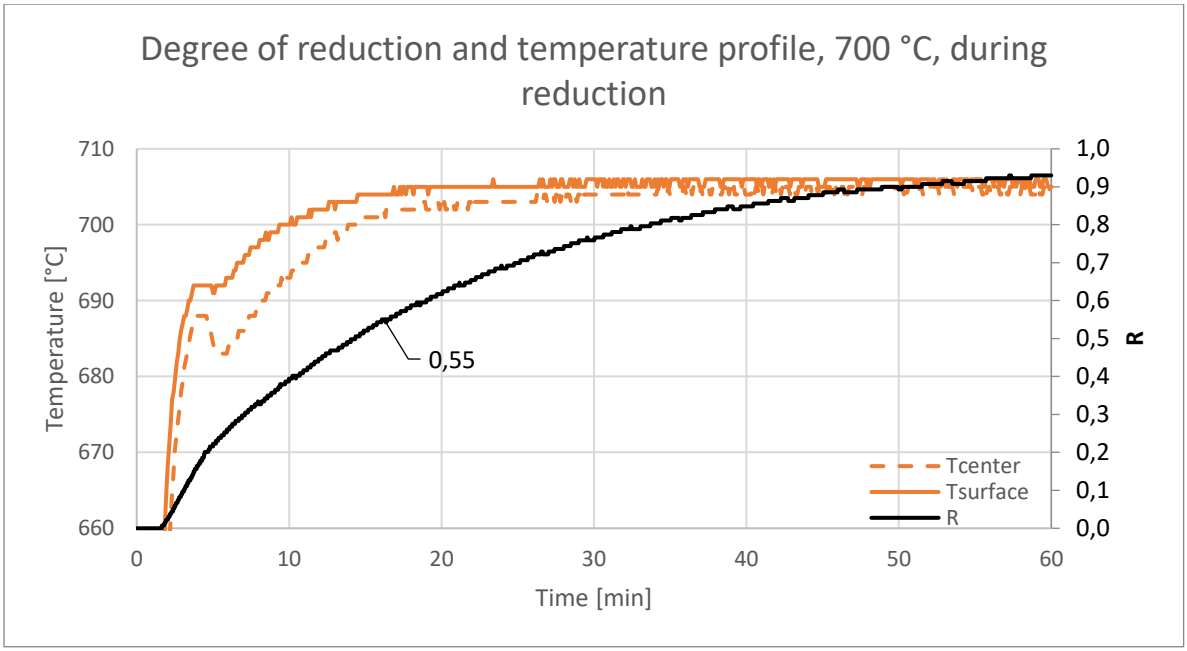

Figure 19, Comparison between the temperature profile during reduction and degree of reduction, 700 °C. The degree of reduction reaches a value of 0.55 before the temperature in the center reaches a steady-state.

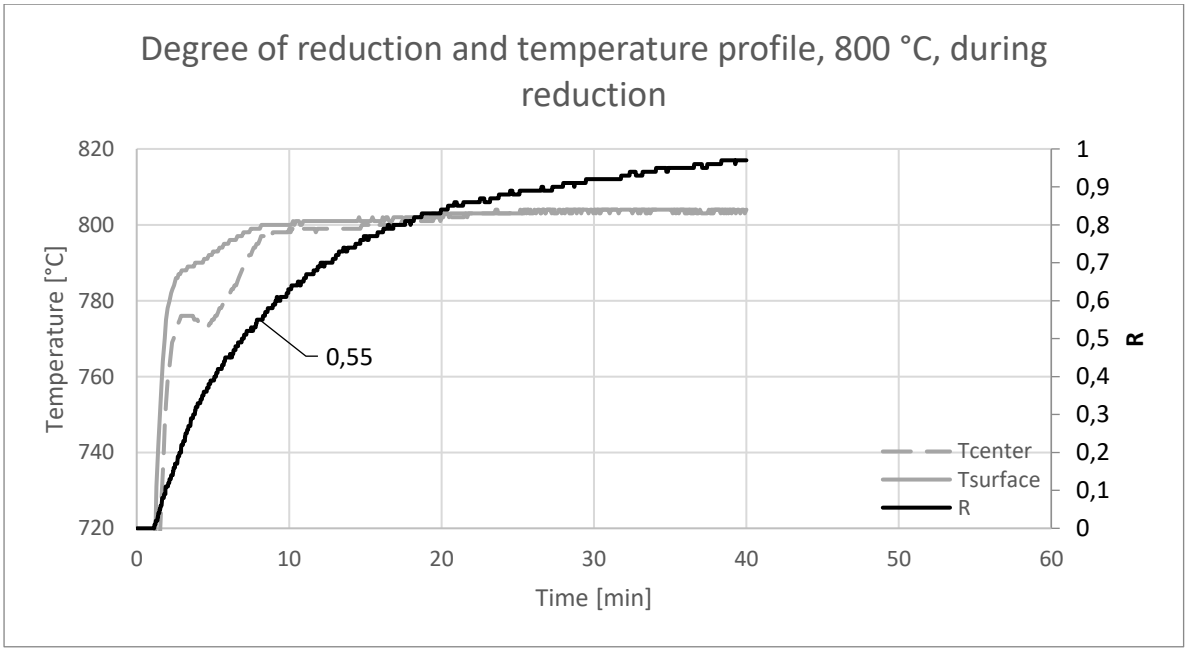

Figure 20, Comparison between the temperature profile during reduction and degree of reduction, 800 °C. The degree of reduction reaches a value of 0.55 before the temperature in the center reaches a steady-state.

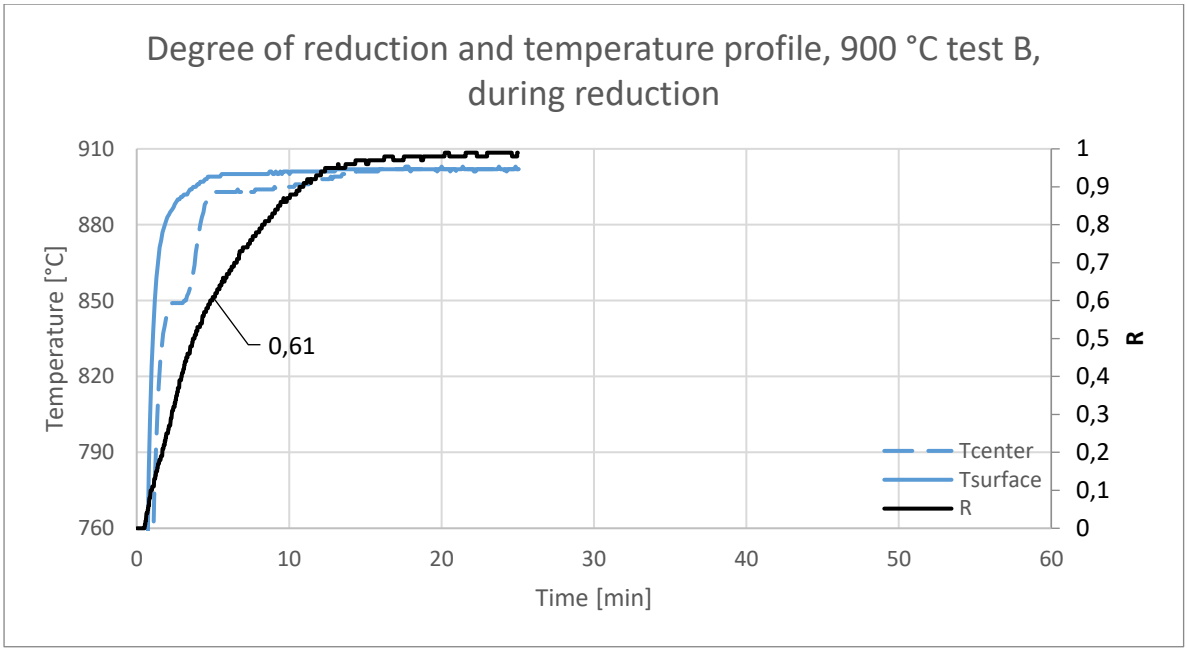

Figure 21, Comparison between the temperature profile during reduction and degree of reduction, 900 °C test B. The degree of reduction reaches a value of 0.61 before the temperature in the center reaches a steady-state.

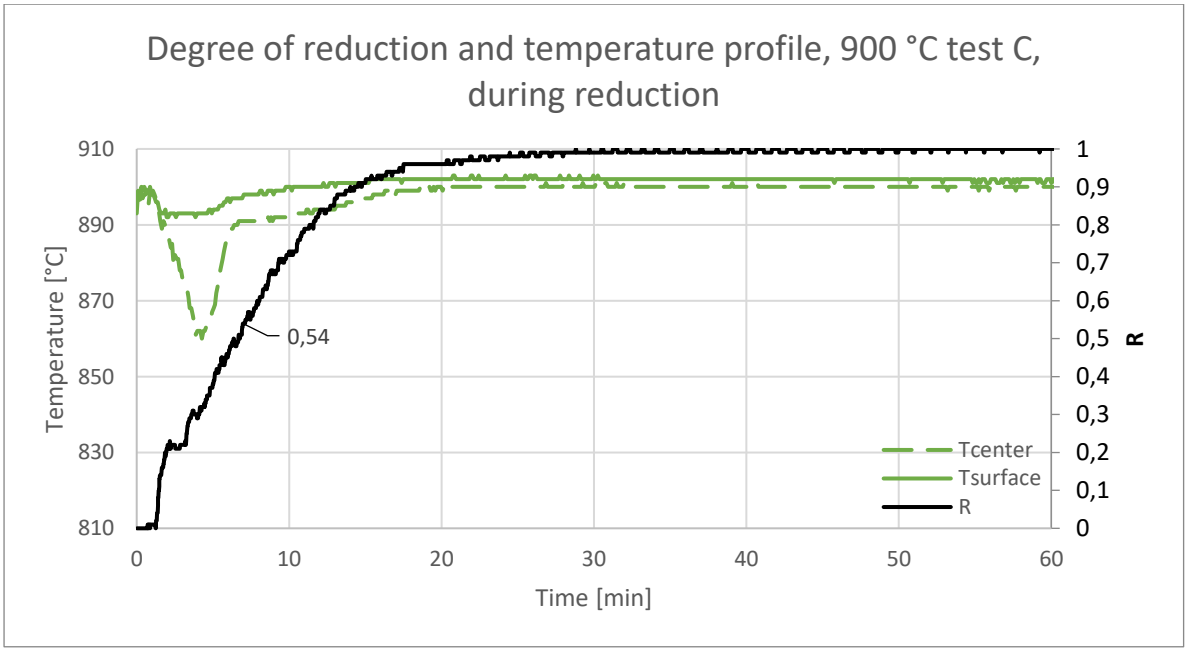

Figure 22, Comparison between the temperature profile during reduction and degree of reduction, 900 °C test C. The degree of reduction reaches a value of 0.54 before the temperature in the center reaches a steady-state.

4.3 CRACKING OF THE HEMATITE PELLETS

Pictures of the pellets, documenting the effects of the hydrogen reduction process are displayed in Figure 23. The reduction process was shown to influence the cracking behavior. At temperatures of 600 °C and 700 °C, Figure 23 a) and b), no or very small cracks could be found at the surface of the pellet after reduction. At the higher temperatures, serious cracks were visible and both the pellet reduced at *800 °C* and *900 °C test C* had cracked to that degree that the pellet fell apart when it was lifted out of the basket, Figure 23 c) and f).

Xu et al. found that both the reduction of Fe_2O_3 and the transformation of SiO_2 are causing cracking in iron oxide pellets, reduced in high reduction potential atmospheres at high temperatures. They saw cracks at temperatures of 800 °C, 900 °C and 1000 °C. They argue that the reaction rate accelerates with the amount of hydrogen, producing a dense metallic product layer in shorter times. The dense iron layer hinders water vapor to exit the pellet at the same rate at which it is produced, thus, the gas pressure makes the pellet crack [37]. Looking at Figure 23, the pellets cracked at temperatures from 800 and 900 °C agreeing to the results of Xu et al.

However, it was expected to find a larger reaction rate constants and a larger rate of reaction, due to the formed cracks. Looking at the reduced *900 °C test C* pellet in Figure 23 f), it would be expected to find it to have a larger rate coefficient than for the *900 °C* test A experiment, Figure 23 d), since that pellet had cracked but did not fall apart. As seen in Figure 14 the *900 °C* test A reaches a higher degree of reduction than the *900 °C test C* until 16 min has passed, R=0.93. After that, the slope of the 900 °C test A curve decreases, as the 900 °C test C curve intersects it and reaches a higher final degree of reduction. However, from these handfuls of results, it is difficult to draw a conclusion about whether the occurrence of cracks widely affects the rate of reaction or not.

Important to remember is that the pellets are to be filled at the top of a shaft furnace and reduced on its way down, the reducing gas and pellets have a counter-current flow. Similarly, to the experiments, the reduction in the shaft furnace will be non-isothermal. As seen in Eq. 2, the reaction rate depends on the pressure of H_2 in the gas stream. If the pellet would crack and separate inside the shaft furnace, it would lead to bad permeability and limit the diffusivity of the reducing gas. It is necessary to perform further experiments to evaluate at which temperature the cracking is small, and the degree of reduction reaches sufficient values. Examining the mechanical strength and the degree of cracking is therefore necessary to understand and include in future processes.

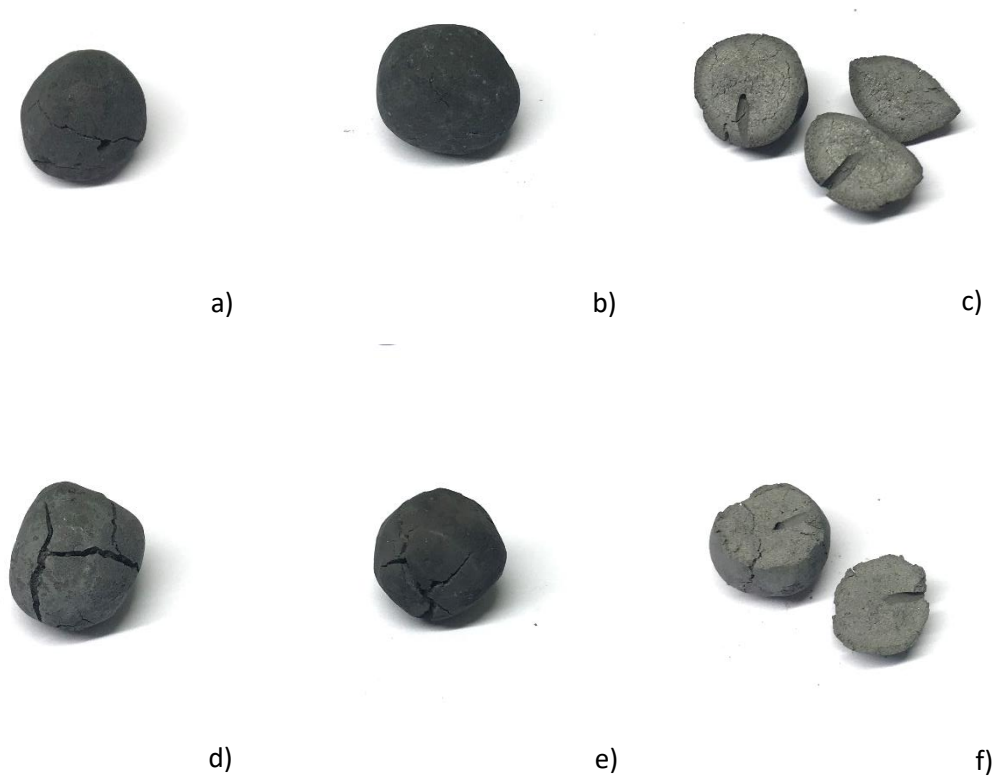

Figure 23, Pictures of the reduced pellet at different temperatures; a) 600 °C, b) 700 °C, c) 800 °C, d) 900 °C test A, e) 900 °C test B and f) 900 °C test C.

5 SUMMARY AND CONCLUSIONS

Experiments were conducted to measure the temperature profile inside hematite pellets during reduction by hydrogen gas. The temperature measurement consisted of two thermocouples placed in the center and at the surface of the pellet, measuring the temperature change during reduction. The standard enthalpy of reaction was calculated for both the carbon-based and hydrogen-based reduction and was found to be: -10 211 [J/mole CO] and +24 282 [J/mole H_2], respectively. From this simple calculation, it is clear that hydrogen-based reduction is an endothermic reaction and therefore it is expected to find a temperature difference between the surface and the center of the pellet. The effect of temperature on the reduction behavior was examined by the application of various temperatures. Four different temperatures were used: 600 °C, 700 °C, 800 °C and 900 °C.

Comparing the temperature profiles before and after reduction with the temperature during reduction, their appearance is totally different. The temperature profile during reduction shows a plateau for the temperature measurement in the center of the pellet and is due to the endothermic reaction taking place. This plateau is seen in all experiment, at all temperatures, and continue longer times for the lower temperatures. At the plateau, the heat consumption is equal to the heat transferred to the reaction zone through a diffuse iron/wüstite layer in the pellet. The apparent thermal conductivity, giving the heat transferred to the reaction site, affects the reaction rate. Higher temperatures increase the temperature difference between the surface and the center, and this in turns affects the reaction rate. At 900 °C, the largest temperature difference was measured, 39 °C. At 800 °C, 700 °C and 600 °C the measured temperature difference was: 18 C°, 9 C° and 3 °C, respectively. The reaction rate increases with temperature and concentration of H_2.

Calculating the ratio between the reaction rate constant for the pellet reduced at 900 °C at the surface and the center gives a 9 times larger reaction rate constant at the surface than at the center. Higher temperatures also gives a larger degree of reduction before the temperature in the center reaches a steady-state: 600 °C R=0.41 and 900 °C R=0.57, proving that it is of high importance to know and understand the temperature profile inside a hematite pellet during hydrogen reduction to be able to simulate the behavior of a pellet inside a large reactor.

The results prove that after a certain initial stage, gas diffusion and heat conduction through the product layers play important roles in controlling the reaction rate. There is even a period where a plateau of the reduction is observed, the reaction is mostly controlled by heat transfer.

6 SUGGESTIONS FOR FUTURE WORK

Some suggestions for the future works and studies are listed down under:

- Examine more pellets reduced during non-isothermal conditions, to be able to draw some conclusions on the cracking behavior. Is there an optimum size of the pellet and reduction temperature, to minimize the degree of cracking?
- Examine the effect on the temperature profile inside a small reactor, reducing a number of pellets at the same time. What does the temperature profile look like inside a pellet placed together with a number of other hematite pellets inside a reactor?
- Examine the effect on the temperature profile during reduction using a combination of hydrogen and carbon monoxide gas. What will the temperature profile look like? Will it contain a plateau or not?

7 ACKNOWLEDGMENTS

I wish to thank my supervisor Ph.D. student Oscar Hessling at the Dept. of Material Science and Engineering at KTH, for the support during my experiments and writing this report. Moreover, I wish to thank Prof. Emeritus Du Sichen for his supervision and mentorship and the countless of hours of discussion and wise words. I would also like to thank Prof. Pär Jönsson, Dr. Johan Martinsson and the group at the end of the hall, Ph.D. students Joar Huss, Amanda Vickerfält, Martin Berg and Jonas Svantesson, at Dept. of Material Science and Engineering at KTH, for all the encouraging words and help during this thesis work. Finally, a big thank you to Magnus Tottie, Manager Product Development at Metlab LKAB in Luleå and LKAB for allowing me to conduct this thesis work.

8 REFERENCES

[1] Naturvårdsverket (Swedish Environmental Protection Agency), "Reduced Climate Impact," 17 May 2019. [Online]. Available: http://www.naturvardsverket.se/Miljoarbete-i-samhallet/Sveriges-miljomal/Miljokvalitetsmalen/Begransad-klimatpaverkan/.

[2] SSAB, LKAB, Vattenfall & HYBRIT development AB, "HYBRIT brochure. Summary of findings from hybrit pre-feasibility study 2016-2017," SSAB, Stockholm, 2018.

[3] C. (. Xu and D.-q. Cang, "A brief overview of low CO2 emission technologies for iron and steel making," *Journal of Iron and Steel Research, International,* vol. 17, no. 1, pp. 1-17, 2010.

[4] D. Gao, M. Hu, C. Pu, B. Xiao, Z. Hu, S. Lui, W. Xun and X. Zhu, "Kinetics and mechanisms of direct reduction of iron ore-biomass composite pellets with hydrogen gas," *International Journal of Hydrogen energy,* vol. 40, no. 1, pp. 4733-4740, 2015.

[5] P. K. Strangwa, S. Toppis and H. U. Ross, "A Study of the Reduction Temperature Obtained During the Isothermal Reduction of Iron Ores," *Canadian Metallurgical Quarterly,* vol. 5, no. 3, pp. 211-219, 1966.

[6] A. Ranzani da Costa, D. Wagner and F. Patisson, "Modelling a new low CO2 emissions, hydrogen steelmaking process," *Journal of Cleaner Production,* vol. 46, no. Key Elements (Stages and Tools) for a Sustainable World, pp. 27-35, 2013.

[7] H. y. Sohn, "Suspension Hydrogen Reduction of Iron Ore Concentrate," American Iron and Steel Institute, Salt Lake City, Utah, 2008.

[8] R. Takahashi, J.-i. Yagi and Y. Omori, "Reduction Rate of Iron Oxide Pellets with Hydrogen," *Science reports of the Research Institutes, Tohoku University. Ser. A, Physics, chemistry and metallurgy,* vol. 23, no. 1, pp. 9-30, 1971.

[9] T. Zhang, C. Lei and Z. Qingshan, "Reduction of fine iron ore via a two-step fluidized bed direct reduction process," *Powder Technology,* vol. 254, no. 1, pp. 1-11, 2014.

[10] M. Kazemi, M. Saffari Pour and D. Sichen, "Experimental and Modeling Study on Reduction of Hematite Pellets by Hydrogen Gas," *Metallurgical and Materials Transactions B,* vol. 48, no. 2, pp. 1114-1122, 2017.

[11] M. Kazemi, "Fundamental Studies Related to Gaseous Reduction of Iron Oxide," KTH Royal Institute of Technology, Stockholm, 2012.

[12] R. Beheshti, J. Moosberg-Bustnes and R. E. Aune, "Modelling and Simulation of Isothermal Reduction of a Single Hematite Pellet in Gas Mixtures of H2 and CO," in *The Minerals, Metals & Materials Society (eds) TMS*, San Diego, CA, United states, 2014.

[13] E. T. Turkdogan and J. V. Vinters, "Gaseous Reduction of Iron Oxides: Part I. Reduction of Hematite in Hydrogen," *Metallurgical and Materials Transactions B,* vol. 2, no. 11, pp. 3175-3188, 1971.

[14] S. Dutta and G. A., "Study of Nonisothermal Reduction of Iron Ore-Coal/Char Composite Pellet," *Metallurgical and Materials transactions B,* vol. 25B, no. 1, pp. 15-26, 1994.

[15] R. Cyprès and C. Soudan-Moinet, "Pyrolysis of coal and iron oxides mixtures. 1. influence of iron oxides on the pyrolysis of coal," *Fuel,* vol. 59, no. 1, pp. 48-54, 1980.

[16] R. Cyprès and C. Soudan-Moinet, "Pyrolysis of coal and iron oxides mixtures. 2. Reduction of iron oxides," *Fuel,* vol. 60, no. 1, pp. 33-39, 1981.

[17] Y. Hara, M. Tsuchiya and S.-i. Kondo, "Intraparticle Temperature of Iron-Oxide Pellet during the Reduction," *Tetsu-to-Hagané ,* vol. 60, no. 1, pp. 1261-1270, 1974.

[18] K. Sato, Y. Nishikawa and I. Tamura, "Pressure Increase and Temperature Fall within a Hematite Sphere during Reduction by Hydrogen," *Tesu-to-Hagane,* vol. 69, no. 9, pp. 1137-1144, 1983.

[19] Y. Man, J. Feng, F. Li, Q. Ge, Y. Chen and J. Zhou, "Influence of temperature and time on reduction behavior in iron ore-coal composite pellets," *Powder Technology,* vol. 256, no. 1, pp. 315-366, 2014.

[20] Y. Man and J.-x. Feng, "Effect of iron ore-coal pellets during reduction with hydrogen and carbon monoxide," *Powder Technology,* vol. 301, no. 1, pp. 1213-1217, 2016.

[21] T. Deng, P. Nortier, M. Ek and D. Sichen, "Limestone Dissolution in Converter Slag at 1873 K (1600 C)," *Metalluurgical and materials transactions B,* vol. 44, no. B, pp. 98-105, 2012.

[22] D. Wagner, O. Devisme, F. Patisson and D. Ablitzer, "A Laboratory Study of the Reduction of Iron Oxides by Hydrogen," *Proceedings of TMS,* vol. 2, no. 1, pp. 111-120, 2008.

[23] E. Kawasaki, J. Sanscrainte and T. J. Walsh, "Kinetics of Reduction of Iron Oxide With Carbon Monoxide and Hydrogen," *A.I.Ch.E Journal,* vol. 8, no. 1, pp. 48-52, 1962.

[24] S. Sun and W.-K. Lu, "A theoretical investigation of kinetics and mechanisms of iron ore reduction in an ore coal composite," *ISIJ International,* vol. 39, no. 2, pp. 123-129, 1999.

[25] M. Kazemi, B. Glaser and D. Sichen, "Study on Direct Reduction of Hematite Pellets Using a New TG Setup," *Steel research Institute,* vol. 85, no. 4, pp. 718-728, 2014.

[26] O. M. Fortini and R. J. Fruehan, "Rate of Reduction of Ore-Carbon composites: Part II. Modeling of Reduction in Extended Composites," *Metallurgical and materials transactions B,* vol. 36B, no. 1, pp. 709-717, 2005.

[27] Y. K. Rao, "A physico-chemical model for reactions between particulate solids occurring through gaseous intermediates- I. Reduction of hematite by carbon," *Chemical Engineering Science,* vol. 29, no. 1, pp. 1435-1445, 1974.

[28] R. H. Tien and E. T. Turkdogan, "Mathematical analysis of reactions in metal oxide/carbon mixtures," *Metallurgical Transactions B,* vol. 8, no. 1, pp. 305-313, 1977.

[29] E. Donskoi and S. Mcelwain, "Mathematical modelling of non-isothermal reduction in highly swelling iron ore-coal char composite pellet," *Ironmaking & Steelmaking,* vol. 28, no. 5, pp. 384-389, 2001.

[30] R. H. Spitzer, F. S. Manning and W. O. Philbrook, "Mixed-Control Reaction Kinetics in the Haseous Reduction of Hematite," *The Metallurgical Society of AIME,* vol. 236, no. 1, p. 726, 1966.

[31] J.-m. Pang, P.-m. Guo and P. Zhao, "Reduction Kinetics of Fine Iron Ore Powder in Mixtures of H2-N2 and H2-H2O-N2 of Fluidized Bed," *Journal of Iron and Steel reasearch, international,* vol. 22, no. 5, pp. 391-395, 2015.

[32] F. J. Plaul, C. Böhm and J. L. Schenk, "Fluidized-bed technology for the production of iron products for steelmaking," *Journal of the Sourthern African Institute of Mining and Metallutgy,* vol. 109, no. 1, pp. 121-128, 2009.

[33] J. L. Schenk, "Recent status of fluidized bed technologies for producing iron input materials for steelmaking," *Particuology,* vol. 9, no. 1, pp. 14-23, 2011.

[34] A. W. Coats and J. P. Redfern, "Thermogravimetric analysis. A review," *Analyst,* vol. 88, no. December, pp. 906-924, 1963.

[35] D. R. Stull and H. Prophet, JANAF Thermochemical Tables, 2nd ed., Washingtin, D.C.: U.S. Department of Commerce, 1971.

[36] L. Minfa, "Gas quenching with air products' Rapid gas quenching gas mixtures," Air products and Chemicals, Inc., Allentown, PA , 2007.

[37] R.-s. Xu, J.-l. Zhang, H.-b. Zuo, K.-x. Jiao, Z.-w. Hu and X.-d. Xing, "Mechanisms of Swelling of Iron Ore Oxideized Pellets in High Reduction Potential Atmosphere," *Journal of iron and steel research, International,* vol. 22, no. 1, pp. 1-8, 2015.

APPENDICES

APPENDIX 1: TEMPERATURE PROFILES, COMPARISON BETWEEN THE TWO 900 °C RUNS

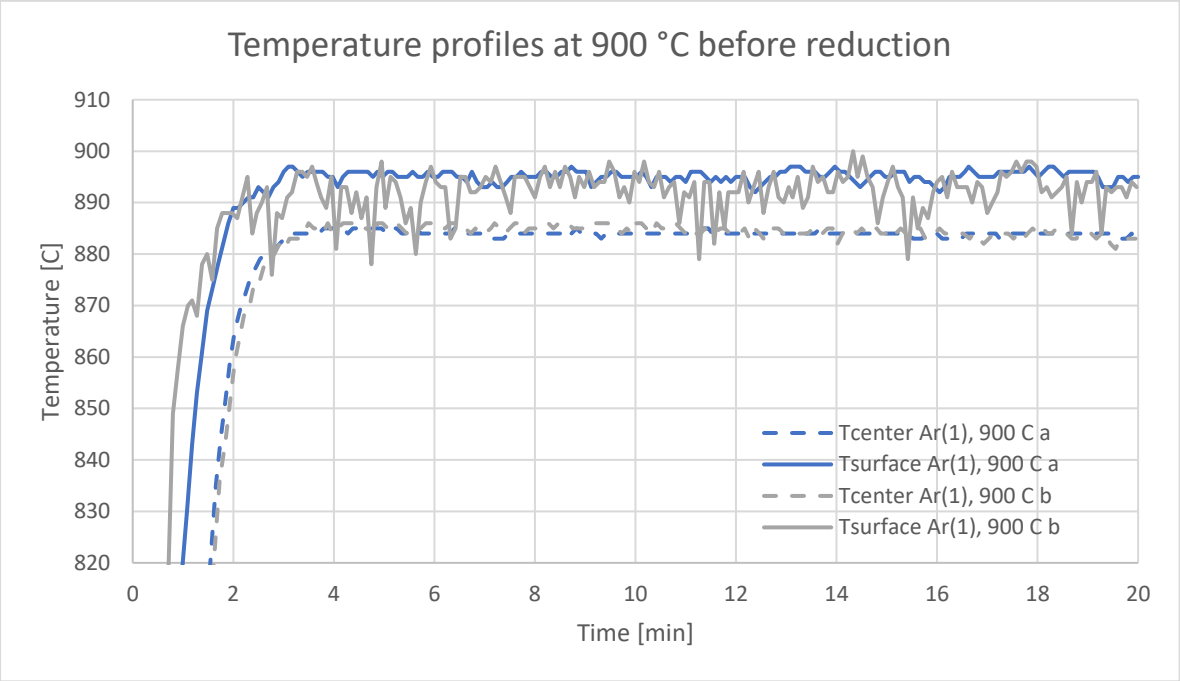

Figure 24, Comparison between the two runs at 900 C, before reduction. The blue lines represent the results from 900 °C test A, and the grey lines represent the results from 900 °C test B.

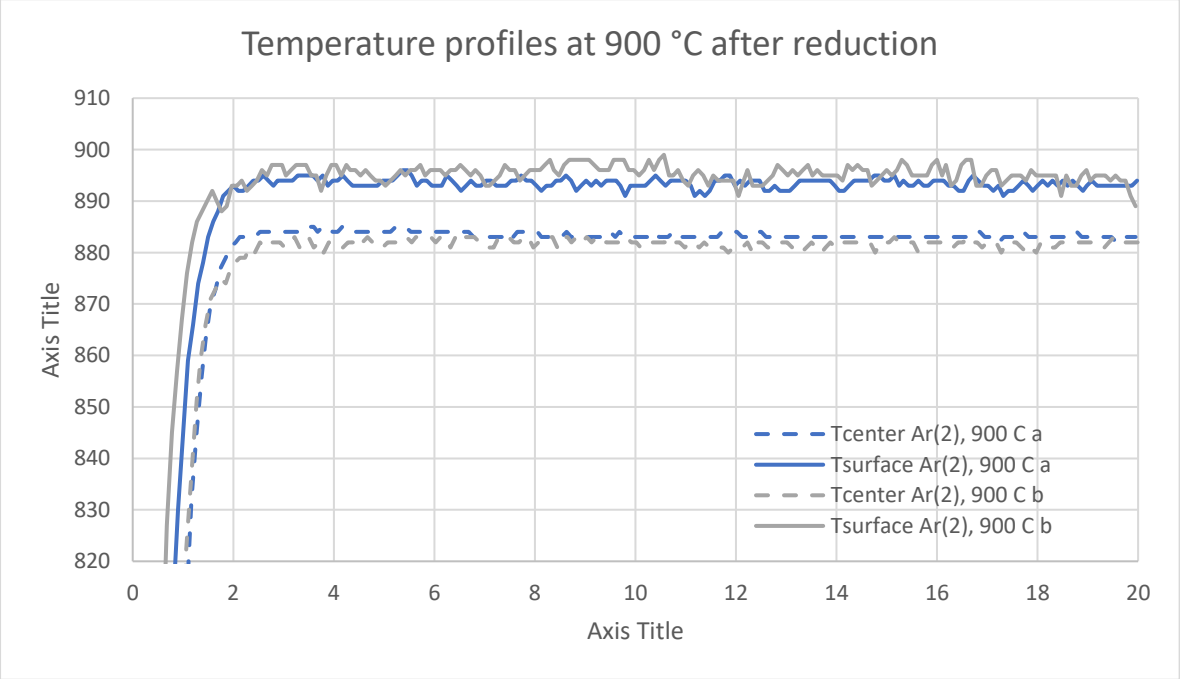

Figure 25, Comparison between the two runs at 900 C, after reduction. The blue lines represent the results from 900 °C test A, and the grey lines represent the results from 900 °C test B.

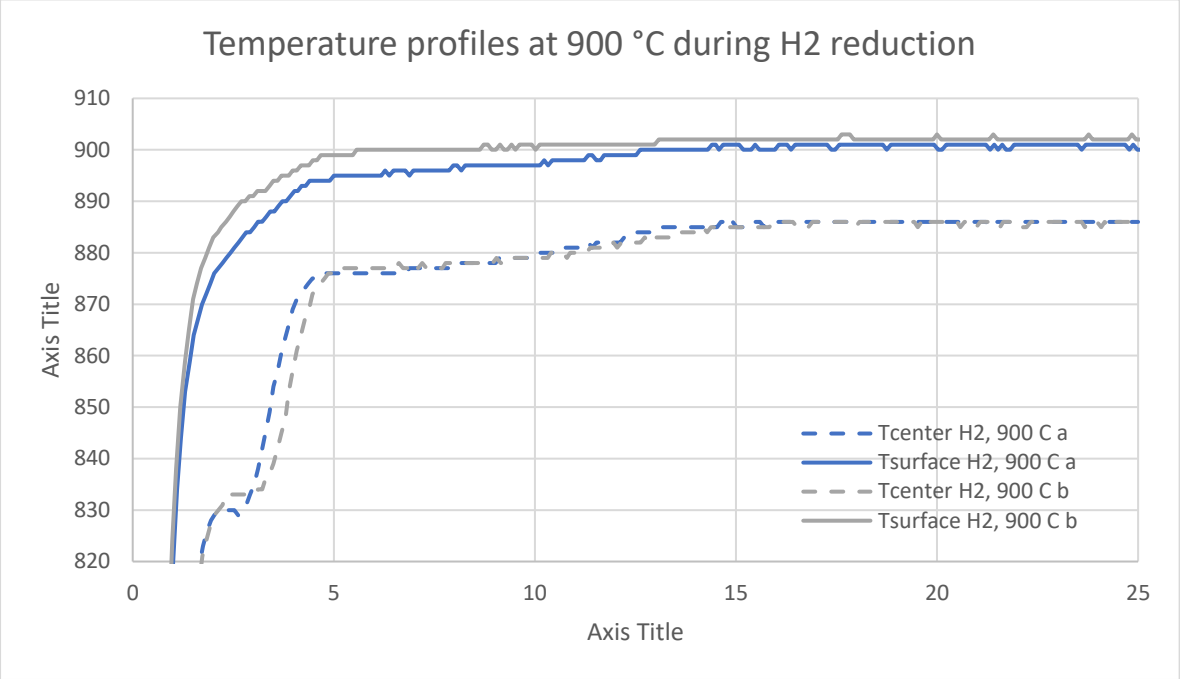

Figure 26, Comparison between the two runs at 900 C, reduction with hydrogen gas. The blue lines represent the results from 900 °C test A, and the grey lines represent the results from 900 °C test B.

TRITA ITM-EX 2019:658